

BRNO UNIVERSITY OF TECHNOLOGY

Faculty of Mechanical Engineering

MASTER'S THESIS

Brno, 2018

Bc. Tomáš Martinek





# **BRNO UNIVERSITY OF TECHNOLOGY**

VYSOKÉ UČENÍ TECHNICKÉ V BRNĚ

## **FACULTY OF MECHANICAL ENGINEERING**

FAKULTA STROJNÍHO INŽENÝRSTVÍ

## **INSTITUTE OF MANUFACTURING TECHNOLOGY**

ÚSTAV STROJÍRENSKÉ TECHNOLOGIE

# **DESIGN OF A NON-RESONANT GENERAL PURPOSE SAMPLE HOLDER FOR TERAHERTZ ELECTRON PARAMAGNETIC RESONANCE SPECTROSCOPY**

NÁVRH NEREZONANČNÍHO DRŽÁKU VZORKU PRO OBECNÉ POUŽITÍ V TERAHERTZOVÉ  
ELEKTRONOVÉ SPINOVÉ REZONANČNÍ SPEKTROSKOPII

## **MASTER'S THESIS**

DIPLOMOVÁ PRÁCE

### **AUTHOR**

AUTOR PRÁCE

**Bc. Tomáš Martinek**

### **SUPERVISOR**

VEDOUCÍ PRÁCE

**Ing. Petr Neugebauer, Ph.D.**

**BRNO 2018**



# Specification Master's Thesis

Department: Institute of Manufacturing Technology  
Student: **Bc. Tomáš Martinek**  
Study programme: Mechanical Engineering  
Study branch: Production of Automotive and Technical Lights  
Leader: **Ing. Petr Neugebauer, Ph.D.**  
Academic year: 2017/18

Pursuant to Act no. 111/1998 concerning universities and the BUT study and examination rules, you have been assigned the following topic by the institute director Master's Thesis:

## **Design of a Non-Resonant General Purpose Sample Holder for Terahertz Electron Paramagnetic Resonance Spectroscopy**

### **Concise characteristic of the task:**

The aim of this MSc thesis is to develop general purpose non-resonant sample holder for broadband Electron Paramagnetic Resonance spectrometer based on THz rapid frequency scans (THz-FRaScan-EPR). Thanks to the developed sample holder the THz-FRaScan-EPR spectrometer will allow multi-frequency relaxation studies of variety of samples ranging from oriented bulk (crystal) materials, over powdered samples to air sensitive samples and liquid solutions. The sample holder should primary operate at frequencies between 80 GHz to 1100 GHz, at temperatures from 1.8 K to 300 K and at magnetic field up to 16 T, capable to perform Far Infrared studies in future.

### **Goals Master's Thesis:**

- Design of general purpose sample holder for compressed powders (5 mm pellets), liquids and oriented single crystals, operating at frequency range 80 GHz – 1200 GHz, with the central frequency set to 430 GHz; temperature range of 1.8 K – 300 K; magnetic fields up to 16 T.
- Design of feeder (carousel) for 5 mm pellets.
- Design of single crystal rotator with the angular resolution better than 2°.
- CST simulation of the radiation coupling to sample holders from a correlated waveguide.

### **Recommended bibliography:**

HARNA, Zdeněk. Přesná mechanika. Brno: Vysoké učení technické, 1996. 148 s. ISBN 80-214-07-4-8.

GOLDSMITH, Paul F. Quasioptical systems: Gaussian beam quasioptical propagation and applications. Piscataway, NJ: IEEE Press, c1998, 430 s. ISBN 978-0-7803-3439-7.

WEIL, John A., James R. BOLTON a John E. WERTZ. Electron paramagnetic resonance: elementary theory and practical applications. 2nd ed. Hoboken, N.J.: Wiley-Interscience, c2007, 688 s. ISBN 978-0-471-75496-1.

Deadline for submission Master's Thesis is given by the Schedule of the Academic year 2017/18

In Brno,

L. S.

---

prof. Ing. Miroslav Píška, CSc.  
Director of the Institute

---

doc. Ing. Jaroslav Katolický, Ph.D.  
FME dean

## ABSTRACT

The aim of this diploma thesis is to design dedicated sample holders for a high-frequency electron paramagnetic resonance spectroscopy. The main task deals with the development of a user-friendly and fast locking system for connection between microwave waveguide and a sample holder. Two types of sample holders are designed one for loading multiple samples and one for single crystal rotation. Thanks to loading up to 6 samples the overall measurement time is estimated to be reduced more than twice. In the case of the single crystal rotator based on the precise piezoelectric rotator with resistive encoder a milliradian, precision is provided. Both sample holders are designed in such a way that the full automatization can be applied in the measurement.

## KEYWORDS

Terahertz Rapid Frequency Scans (THz-EPR), quasi-optics, Electron Paramagnetic Resonance (EPR) spectroscopy, EPR sample holder, low temperature, high magnetic field, CST studio, waveguides

## ABSTRAKT

Cílem diplomové práce je navrhnout konstrukční řešení držáků vzorků pro vysokofrekvenční elektron paramagnetickou resonanci. Předmětem návrhu je vytvořit jednoduchý zamykací systém pro spojování mikrovlnného vlnovodu a držáku vzorku. Dále navrhnout systém s řešením držáku pro více vzorků. Toto unikátní provedení držáku povede k několikanásobné úspoře celkového času měření vzorků. Poslední návrh spočívá v optimalizaci držáku vzorku s možností naklápění osy, kterou lze díky přímému napojení na piezoelektrický rotátor pootáčet s přesností na miliradiány. Oba typy držáku vzorku jsou navrženy s ohledem na automatizaci měření.

## KLÍČOVÁ SLOVA

Vysokofrekvenční skenování (THz-EPR), kvasioptika, Elektronová paramagnetická resonance (EPR) spektroskopie, EPR držák vzorku, nízká teplota, vysoké magnetické pole, CST Studio, vlnovod

MARTINEK, Tomáš *Design of a Non-Resonant General Purpose Sample Holder for Terahertz Electron Paramagnetic Resonance Spectroscopy*: master's thesis. Brno: Brno University of Technology, Faculty of Mechanical Engineering, Ústav strojírenské technologie, 2018. 70 p. Supervised by Ing. Petr Neugebauer, Ph.D.





## DECLARATION

I declare that I have elaborated my master's thesis on the theme of "Design of a Non-Resonant General Purpose Sample Holder for Terahertz Electron Paramagnetic Resonance Spectroscopy" independently, under the supervision of the master's thesis supervisor and with the use of technical literature and other sources of information which are all quoted in the thesis and detailed in the list of literature at the end of the thesis.

Brno .....

.....

(author's signature)



## Acknowledgment

There are many people who contributed to this work, or just helped me to go through my studies. I can consider myself very lucky that I have met such a number of talented and friendly people everywhere life has taken me.

I would like to thank my supervisor Ing. Petr Neugebauer, Ph.D. for introducing me to the electron paramagnetic resonance, his friendly advice, and guidance at all times. My special thanks belong to Ing. Antonín Sojka for his expertise and patience at all times. His advice and support have been invaluable. I would like to extend my sincere gratitude to my friends and colleagues at the CEITEC MOTES.

And last but not least, I am grateful for the encouragement my parents, my brother and my sister have given me. It would not have been possible to write this thesis without the help and support of the kind people around me.

Bc. Tomáš Martinek



# CONTENTS

<b>Introduction</b>	<b>1</b>
<b>1 Introduction to Electron Paramagnetic Resonance</b>	<b>3</b>
1.1 Overview . . . . .	3
1.2 Historical Aspect . . . . .	3
1.3 Commentcement of NMR in Brno . . . . .	4
1.4 EPR Principle . . . . .	6
1.5 Why High Field/Frequency EPR Spectroscopy . . . . .	8
<b>2 EPR Spectrometer</b>	<b>11</b>
2.1 Microwave Source . . . . .	11
2.2 Quasioptical Propagation System . . . . .	11
2.2.1 Oversized (Corrugated) Waveguide . . . . .	13
2.2.2 Corrugated Taper . . . . .	13
2.3 Sample Holder (Cavity) . . . . .	13
2.3.1 non-resonance Sample Holder . . . . .	15
2.3.2 Rotating Sample Holder . . . . .	16
2.4 Magnet and Cryostat . . . . .	16
2.5 Detector . . . . .	17
2.6 Computer Controler . . . . .	17
<b>3 Quasioptics</b>	<b>19</b>
3.1 Gaussian Beam . . . . .	19
3.2 Inverse Formulas for the Gaussian Beam . . . . .	20
3.3 Confocal Distance . . . . .	21
3.4 Beam Coupling . . . . .	21
<b>4 Requirements and Constructional Techniques</b>	<b>25</b>
4.1 Construction at Low Temperatures . . . . .	25
4.1.1 Requirements for Sample Holder Design in Low Vacuum Environment . . . . .	25
4.1.2 Desorption of Gasses . . . . .	25
4.1.3 Leakage . . . . .	26
4.1.4 Mechanical Connections . . . . .	26
4.1.5 Cleanliness of Components . . . . .	28
4.2 Selection of Materials for Cryogenic Environment . . . . .	28

<b>5</b>	<b>Multi Propose HF-EPR Sample Holder</b>	<b>31</b>
5.1	The Probe . . . . .	31
5.2	Connection of Sample Holder and Corrugated Taper - Locking System	32
5.2.1	The Flange of Corrugated Taper and Sample Holder . . . . .	34
<b>6</b>	<b>Design of Sample Holders</b>	<b>37</b>
6.1	Carousel Sample Holder . . . . .	37
6.1.1	Selection of Mechanism . . . . .	38
6.1.2	Propulsion of Carousel . . . . .	39
6.1.3	Gears . . . . .	42
6.1.4	Optical Sensor of Position . . . . .	43
6.1.5	Modulation Coil . . . . .	45
6.1.6	Description of Assembling . . . . .	49
6.1.7	Sample Exchange . . . . .	52
6.1.8	Simulation of Gaussian Propagation for Carousel Sample Holder	53
6.2	Rotating Sample Holder . . . . .	55
6.2.1	Description of Assembly . . . . .	56
6.2.2	Propulsion System . . . . .	56
6.2.3	Modulation Coil . . . . .	58
6.2.4	The Sample Exchange . . . . .	59
6.2.5	Simulation of Gaussian Propagation for Rotating Sample Holder	61
	<b>Bibliography</b>	<b>65</b>
	<b>Appendix</b>	<b>71</b>

# INTRODUCTION

The method called Electron Paramagnetic Resonance (EPR) is well known spectroscopy technique to study paramagnetic materials. It is based on the absorption of microwave radiation by sample which contains unpaired electrons. Thanks to this phenomena the information about magnetic properties of the sample such as relaxation times, zero field splitting and more can be obtained from single measurement [1]. Therefore, from its invention the method has gained an irreplaceable place between the physics and chemists.

The aim of this diploma thesis is to develop a design of two unique non-resonant sample holders for EPR spectroscopy. The first sample holder is unique in such a way that it allows to carry up to six samples at once. Compared with the traditional sample holders, which allow to carry only one sample, measuring time necessary to sample exchange will rapidly drop down. Moreover, in new design configuration the reference can be placed, therefore, the spectra background will be easily determined. The second unique sample holder is rotating sample holder. By stacking the crystal on the rotary shaft, the vacancies or crystal defect can be studied [1]. Because the design of each sample holder is first of its kind the simulations were done to assure functionality.

The concept of this thesis can be divided into two main parts. In the first part, four chapters are focusing on a theoretical overview of EPR technique. They are acquired for furthermore understanding of the topic and all problems which are dealt with in second practical part of this thesis.

The first chapter of the thesis introduces the fundamentals of EPR spectroscopy focusing on the history of NMR in Brno. Consequently, the overview of the EPR spectroscopy, elementary theory of Zeeman Effect and its using in a different field of science is discussed.

In the second chapter, attention is paid to certain parts of the spectrometer, such as the microwave bridge, the microwave waveguides, and the sample holders. Furthermore, this chapter describes two most frequently used types of sample holders.

The third chapter introduces the basic theory of microwave radiation and the reason why the quasi-optics (QO) is used for EPR spectroscopy. Moreover, the foundation of Gaussian beam propagation is showed with necessary equations describing the microwaves propagation.

Last chapter of theoretical part of thesis, chapter four, presents the possible problems with the construction of components used at low temperature.

In Chapter five, a new system of general purpose connection between microwave waveguide and the sample holders is described and the handling of the connection

is explained.

At the end, the practical chapter about sample holders follows. Each chapter contains firstly the introduction of the design of both new sample holder types including their advantages and disadvantages. Then, the constructive solution of sample holders is presented and simulation of wave propagation is discussed.

In chapter six, a unique carousel sample holder is presented. The rotary carousel constitutes many advantages for conventional measurement. Thanks to it, it is possible for the EPR spectrometer to contain the reference among the other five samples per the one round of measurement.

The this chapter is dedicated to an improvement of the commonly used rotating sample holder.



# 1 INTRODUCTION TO ELECTRON PARAMAGNETIC RESONANCE

## 1.1 Overview

EPR spectroscopy, sometimes called Electron Spin Resonance (ESR) spectroscopy, is an analytic method to detect, analyse and ascertain unpaired electrons in paramagnetic species such as free radicals or transition metals. This technique is based on the selective absorption of electromagnetic waves by a paramagnetic material placed in an external magnetic field. The basic substance of the EPR method is similar to Nuclear Magnetic Resonance (NMR) [2]. However, in EPR the electron spins are excited in compare to NMR where the excitation is realized on atomic nuclei. Both spectroscopy methods enable to study materials regardless of whether they are in the gaseous, liquid or solid state. It is used by the chemist for a monitoring of chemical reactions, determination of structure and function of biological macromolecules, determine motions of molecules [1].

In a different way, EPR spectroscopy is used by physics. They are using this technique for an observation of crystal vacancies. Moreover, among the most important information obtained from the specter include electric distribution levels in the sample and spin relaxation in single molecules magnets. Nowadays hot topic for developing new data storage and quantum computing [3].

A schematic of basic principle of the most simply EPR spectrometer is depicted in Figure 1.1. It consists of three essential components such as a source of electromagnetic radiation, a sample and a detector [4]. To gain a spectrum, the frequency of the microwave radiation is going to the detector through the sample. In certain condition (will be discussed later) the microwave is absorbed by sample which can be seen in the spectrum as decreasing of the intensity of the signal.

## 1.2 Historical Aspect

The first mention related to the Electron Paramagnetic Resonance dates back to 1920 when the experiment was performed by Stern and Gerlach and their results proved the magnetic moment of the electron can have only distinct orientations [5]. However, the phenomenon of EPR started in Kazan, (USSR, nowadays Russia) at the end of the Second World War, when E. K. Zavoisky carried out the first experiment of EPR. His observation was connected by the experiments of NME of liquids and solid in the field of magnetic resonance. However, the observation was unclear, due to the use of an inhomogeneous magnetic [6]. Due to this experience he

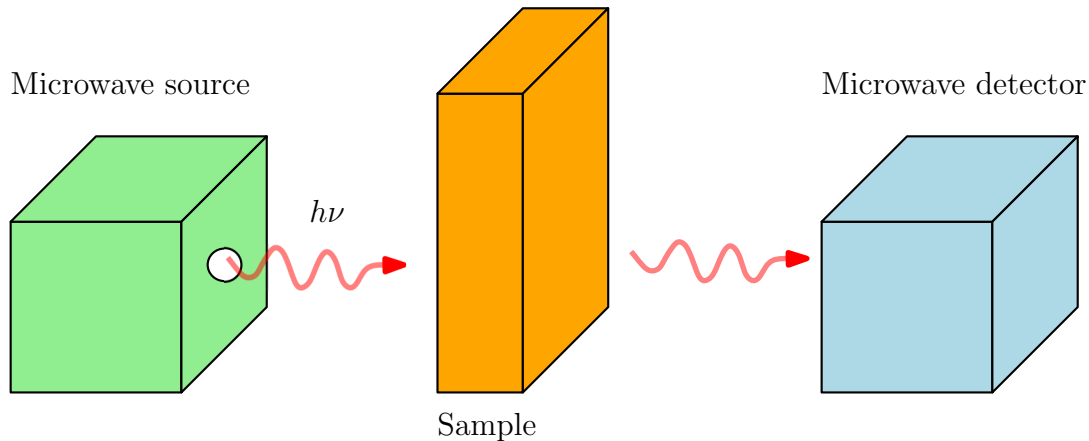


Figure 1.1: The most simply EPR spectrometer. Taken from [4].

focused on EPR, where the inhomogeneous magnetic field can be used. He detected a microwave absorption in a salt sample at a magnetic field of 4,76 mT for a frequency of 133 MHz in 1944 [6]. The design of the first EPR spectrometer, the equipment of RADAR were used. This Zavoisky's establishment made for the British Oxford Group initial point for several reports of theoretical and experimental studies [7].

During the 1980s, the emphasis was given on the research of electron spin and also on the interconnection of physical properties and the material science. This increased the demand of EPR, however, Janzen developed the EPR spin trap method, which took widely utility of EPR in the medical and pharmaceutical field [8].

Another point of view was taken by F. El Hallak, J. van Slageren and M. Dressel in Stuttgart in the year 2010 where they developed and used a macrocantilever. They recorded broadband EPR spectroscopy by capacitive detection of the cantilever and the name of this method is torque detected electron spin resonance. The sample on the cantilever was irradiated by microwaves (see Fig. 1.1) [9].

Nowadays, EPR methods are progressing very fast. Pulsed X-band, Q-band, and W-band spectrometers are made for many commercial applications and pulsed experiments are necessary for many observations. Both techniques, NMR and HF-EPR, start to be combined in the dynamic nuclear polarization of experiments where the polarization of nuclei via electronic cross relaxation is carried out by HF-EPR techniques [10].

### 1.3 Commentcement of NMR in Brno

As a proud student of BUT in Brno, I presume to remind the history of NMR spectroscopy in Brno. The inforamtion is taken from [11].

The Brno's NMR spectroscopy started with a group of fanciers, ahead of J. Dadok, at a Institute of Scientific Instrument (The Czechoslovak Academy of Sciences) in Brno at the end of the 1950s. They were able to design a functional NMR spectrometer. However, further development already took place in cooperation with a company TESLA Brno, which produced electronic components at that time. The new developmental division was established under a direction of A. Sapík. In 1965, TESLA Brno showed the world a new TESLA BS477 (see Figure 1.2) spectrometer with a frequency 60 MHz for a proton, which utilized ten years of experience at the Institute of Scientific Instrument. At that time, TESLA Brno was the third company in the world, which started producing the spectrometers after an American company Varian or a Japan company Jeol.



Figure 1.2: The NMR TESLA BS 477 spectrometer in 1965. Taken from [11].

The further development aimed to shift the boundaries of the spectrometer and improve the level of the measured spectra. Therefore, new upgraded types were followed and took the first successes. TESLA won the gold medal of Brno Fair, and competing companies recognized the quality of the Brno's spectrometers. Moreover, the experts of competing companies came to see, how TESLA produces, for example, pole magnet mounts, which have a major influence on the homogeneity of the external magnetic field. In the 1970s, a company Zeiss began negotiated the cover of demand for NMR spectrometer in the German Democratic Republic (GDR) with TESLA, because the excessive complexity of electronic components in the spectroscopy was beyond the forces of this Swiss company.

During the 1980s, the inconsistency in company management began to emerge, followed by a decline in the development of new spectrometers. There was an offer from a company Bruker, which proposed to supply electronic equipment and TESLA

would implement its highly efficient magnets. This event was finally realized, but it was the last bang for the production of spectrometers in our country. Due to expensive price of Helium, the value of spectrometers decreased and the manufacturing was ended along with the political upheaval in 1989.

However, the history of Brno's NMR spectroscopy is sunk into oblivion currently, albeit, the Czechoslovakian scientific activity brought many achievements and milestones. In honor of the founder (Josef Dadok) of NMR in the Czech kingdom, the J. Dadok National NMR Centre is named after him [11].

## 1.4 EPR Principle

The method of Electron Paramagnetic Resonance is based on the Zeeman Effect (Fig. 1.3). The principle can be explained on a simple electron spin like the hydrogen. The hydrogen contains one electron in  $s$  orbital. At zero magnetic field, the electron energy levels of the two possible spin states ( $m_s = \pm 1/2$ ) are degenerate. However, when we apply an external magnetic field the degeneracy is lifted and the separation of two energy levels can be observed. If the system is irradiated by an electromagnetic wave with exact energy, the incoming wave is absorbed and electron spin is flipped [1].

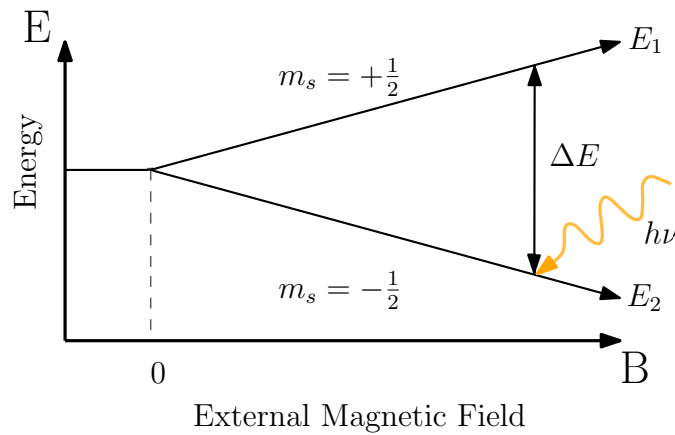


Figure 1.3: Zeeman effect with two states of energy levels. Taken from [1].

The classical EPR spectrometer works as follows. The sample is irradiated constantly by microwave energy while sweeping magnetic field. The absorption of the microwave is observed at the resonance condition:

$$E = h\nu = g\mu_B B \quad (1.1)$$

where  $\nu$  is frequency of incoming wave (photons),  $h = 6,626 \cdot 10^{-34} J \cdot s$  is Planck constant,  $g$  is the Landé g-factor,  $\mu_B = 9,274 \cdot 10^{-28} J \cdot G^{-1}$  is Bohr magneton and  $B$  is the external magnetic field [1].

The peak in EPR spectra can be assigned to absorption of the microwave. However, from equation 1.1 can be seen the only parameter whose value is connected to the sample is the g-factor. The measured spectra then show the absorption at a certain value of MW and magnetic field and therefore the main parameter of interest is g-factor:

$$g = \frac{\nu h}{\beta B_0} \quad (1.2)$$

The EPR spectrometers can work in two modes which follow resonance condition. Sample is irradiated by microwave energy held constant while sweeping magnetic field (field domain).

The magnetic field is kept constant and the sample is irradiated by sweeping frequency (frequency domain). For both modes when resonance condition is met (see equation 1.1) the absorption of the incoming wave occurs. Comparison of field domain and frequency domain spectrum can be seen in Figure 1.4. As can be seen, the spectra are similar. The reason for this phenomena can be explained by the resonant condition. If the measurement is kept in field domain and the magnetic field is kept constant and the energy of microwave is increasing and therefore first peaks in spectra belong to high energy transitions and vice versa.

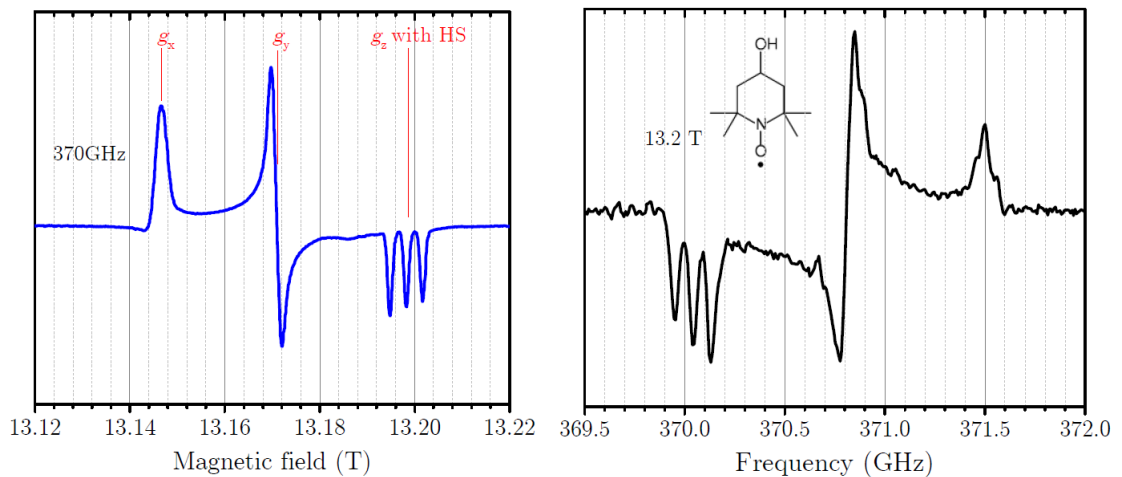


Figure 1.4: Comparison of field domain and frequency domain. Taken from [12].

Up to now, the field domain technique takes first place mainly due to technology requirements. The source able to sweep with the frequency over the broad frequency

range with sufficient efficiency was not developed for last decades. Nowadays, however, thanks to stable microwave sources for EPR the frequency domain EPR starts to play a more important role.

## 1.5 Why High Field/Frequency EPR Spectroscopy

By moving to high frequencies and high magnetic fields, better spectral resolution of radicals and new phenomena can be observed. Parameters of spin Hamiltonian:  $g$ -factor and zero-field splitting (ZFS) parameters, giving information about magnetic properties, can be precisely determined by High Field/Frequency EPR (HF-EPR) [13].

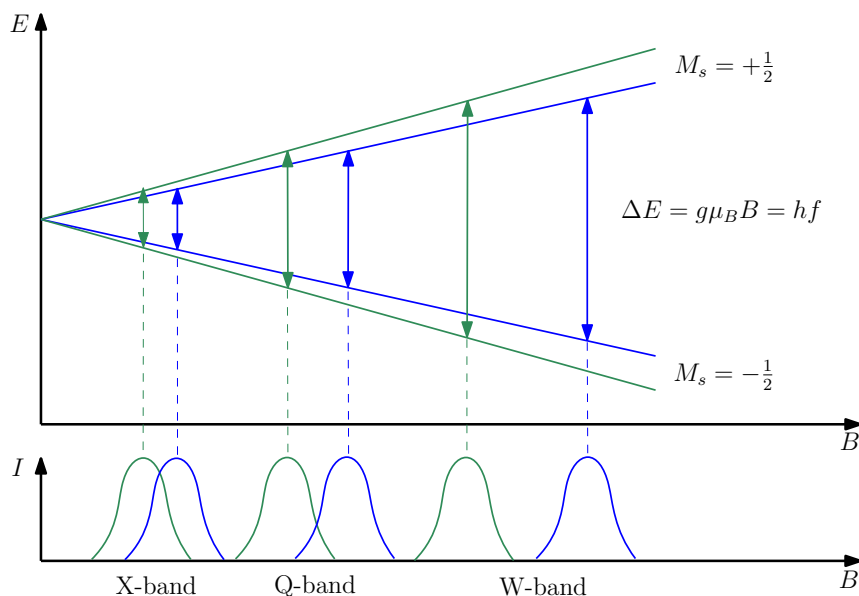


Figure 1.5: A simplified energy level diagram of spin  $S = 1/2$  system with 2 species with different  $g$  values. In the X-band frequency range, they are almost indistinguishable. After applying higher magnetic field and frequency, the separation of levels starts to be bigger and two different  $g$  value can be distinguished. Taken from [14]

The main reason why higher magnetic fields are used is the enhancement of spectral resolution with the increase of magnetic fields and MW frequencies. This can be schematically depicted in Figure 1.5 where two types of different  $g$ -values are shown. In the case of X-band frequencies and even at Q-band frequencies, the resolution of two components can be very difficult to resolve correctly (Figure 1.5).

Due to this fact, a W-band spectrometer can be considered as one order of magnitude higher than that of an X-band spectrometer [13].

Next chapter will provide the brief description of the EPR spectrometer.





## 2 EPR SPECTROMETER

EPR spectrometers have been under development for many years. They reflect progress in various fields of physics, particularly in semiconductor physics for detectors and source of microwaves, and in physics of superconducting materials for magnets. In high field/high frequency electron paramagnetic resonance (HF-EPR) spectroscopy, knowledge of quasioptics (QO) used in astrophysics research. All these innovations and improvements have allowed the increase of frequency or use of pulse operation, as well as enabled a better spectral resolution for systems with small  $g$  anisotropy [14].

For more precise observation of the sample, the more sophisticated EPR spectrometer than is depicted in Figure 1.1 is used. The HF-EPR spectrometer is schematically shown in figure below (Figure 2.1). The spectrometer can be divided into upper and lower part. The upper part contains microwave bridge, where the microwave source, the detector, and QO propagation system are placed. The microwave bridge is often made of an aluminum plate and it is basically support for these mentioned components. The lower part is composed of superconducting magnet, where the sample holder and all necessary components are placed.

The description of the device starts with microwave source, through QO propagation system, continues to magnet and it ends with the characterization of the detector. Described components of EPR spectrometer are going in the same direction as microwave radiation. All these necessary parts of the EPR spectrometer are captured in Figure 2.1.

### 2.1 Microwave Source

For creating electromagnetic microwave the source placed in the microwave bridge of the spectrometer is applied. The older types of EPR spectrometer uses the Gunn diode which is constituted by a monocrystal of arsenide gallium with a conductivity of type N [15]. Nevertheless, the Gunn diodes are replaced by dielectric resonance oscillators. This occurs due to significant improvements of multipliers which allow using higher microwave powers.

### 2.2 Quasioptical Propagation System

The quasioptical propagation system, depicted in figure, consists of the microwave components, which are necessary for direct microwave propagation. The system is constituted by the circulators, phase shifters, mirrors, waveguides, polarizers, and

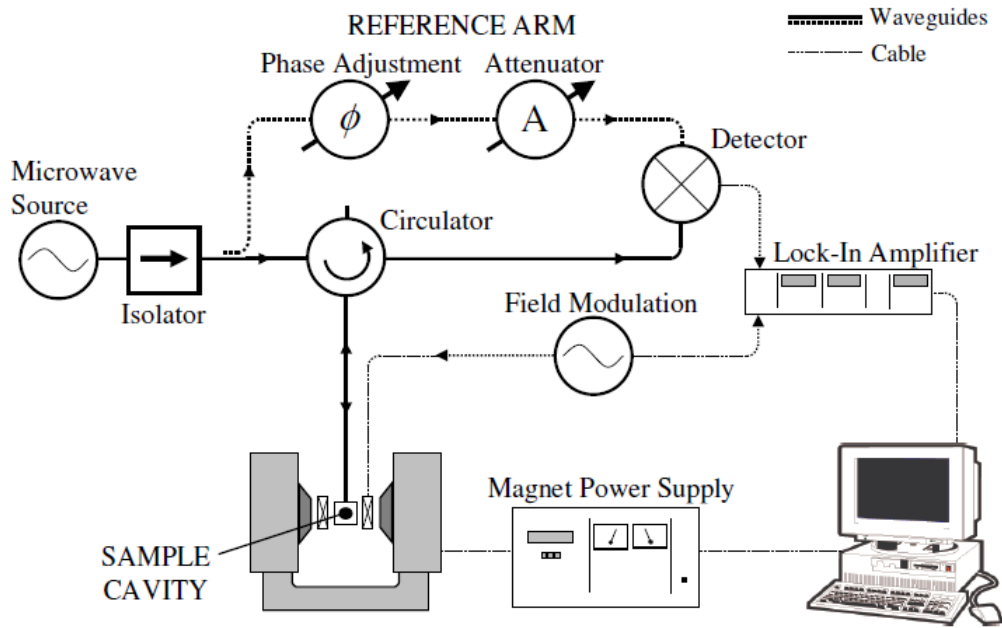


Figure 2.1: Schematic description of the HF-EPR spectrometer with homodyne detector. Single mode rectangular waveguides and other microwaves components placed in the microwave bridge are depicted in figure. The single mode cavity in the center of a resistive magnet is used for a placement of the sample. Taken from [14].

etc. The microwave radiation is propagated in a free-space or in the space with low pressure. The QO free space propagation is employed for microwave propagation in upper part of the spectrometer [16].

Waveguides, one of QO propagation system, can be also used. There are several types of the waveguides. One of them is the single mode rectangular waveguide, which is used up to frequencies 100 GHz, because when it passes over this boundary high losses occur [17], [18].

The next possibilities are oversized or corrugated waveguides. The oversized waveguides, which have smooth surface, have typically lower losses than rectangular waveguides. In contrast, corrugated waveguides have surface with grooves and it is used for negligible losses and for its excellent polarisation purity [19]. The shape of waveguides can be rectangular or circular. The circular shape provides better propagation of microwave radiation [20].

### 2.2.1 Oversized (Corrugated) Waveguide

Due to low losses and suitable phase orientation, the oversized waveguide with a corrugated surface instead of a smooth internal surface inside walls of the waveguide is applied. The depth of the corrugation is  $d = \lambda/4$  with a typical period  $< \lambda/3$ . When the applied wavelength  $\lambda$  is  $\lambda = 4d$  the microwave are propagated with negligible losses [16]. When the frequency increases, the losses can be lower due to the ratio  $\lambda^2/a^3$ , where  $2a$  is the inner diameter of the waveguide. In the circular corrugated waveguide is obtained very great polarisation with extremely good purity, if the  $2a$  diameter is adequately large and  $d \approx \lambda/4$  [19], [21].

Generally, the corrugated waveguides are applied in all modern HF-EPR systems. In the Figure 2.2 the microwave probe and taper is shown, where the corrugations are used. The total length of the microwave probe depends on the parameters of the used magnet. To the conical horn (taper) is connected the sample holder and the major function of the taper is to concentrate the microwave power [22].

### 2.2.2 Corrugated Taper

The conical horn and conical taper (shortly taper) are suitable for cavity design because they allow connecting different cavity designs with very low intersection losses. Horns and tapers are widely used in radar systems [16]. Their manufacturing is usually performed by electroforming technique, when the cooper is applied on an aluminium mandrel. The mandrel is subsequently etched away [23]. The sense of this technique deals with the machining of outer aluminium mandrel instead the inner surface of conical horn (taper).

## 2.3 Sample Holder (Cavity)

The resonant cavity is employed in conventional EPR, to maximize interaction of the microwave radiation with the sample and it is simply a box with a rectangular or cylindrical shape made from metal, quartz or polymeric material [22]. Resonance causes the amplification of microwave energy in the cavity, when the resonance condition is achieved. Simple implementation of resonance cavity is Fabry-Pérot resonator, which acts as bandpass filter for microwaves. The size of resonator depends on the wavelength  $\lambda$  [22].

The quality factor  $Q$  expresses the amount of stored microwave energy, it is the efficiency cavity. By increasing the  $Q$ , the sensitivity of the spectrometer increases too [4].

$$Q = \frac{2\pi(\text{energy stored})}{\text{energy dissipated per cycle}} \quad (2.1)$$

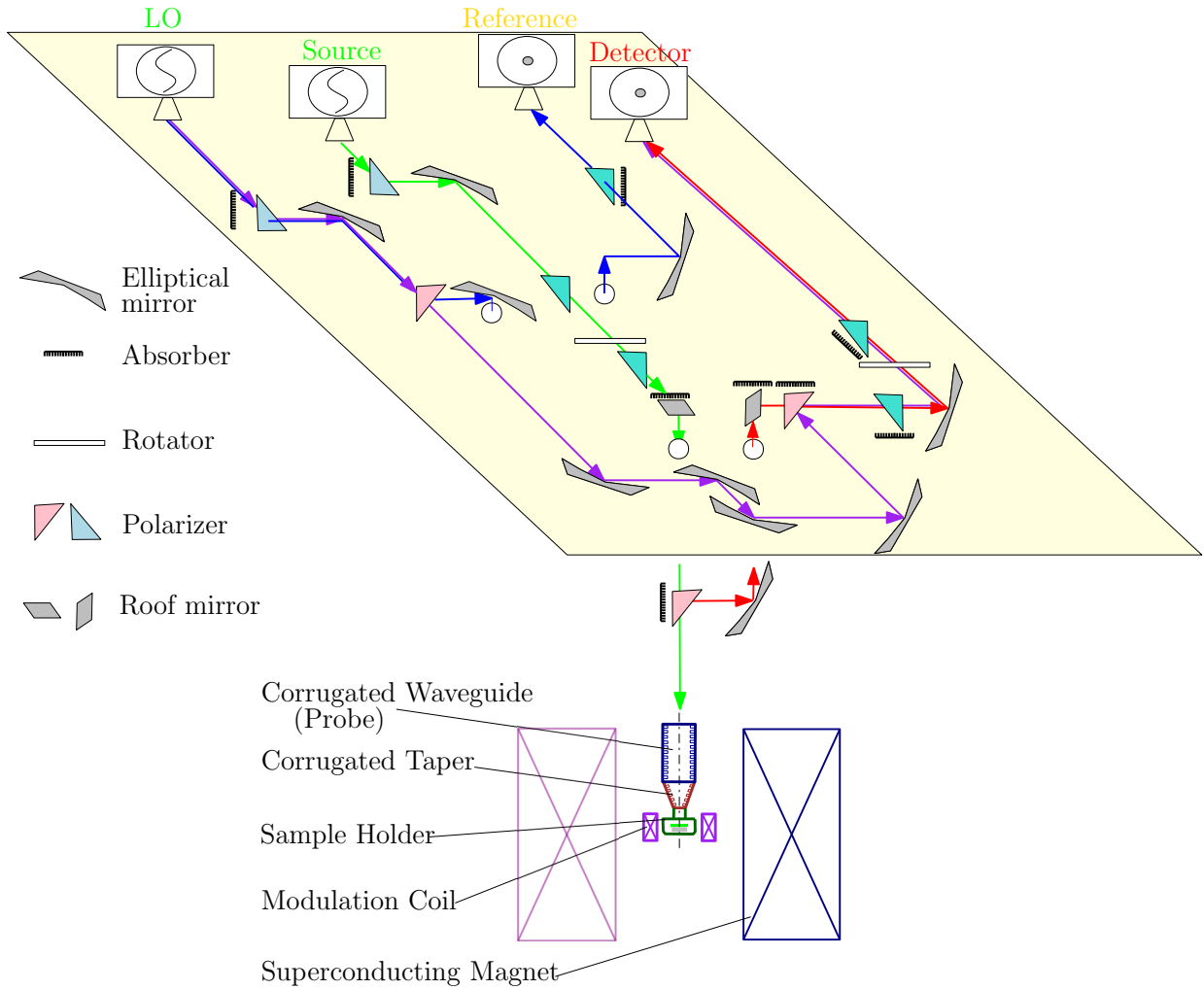


Figure 2.2: The schematic description of the HF-EPR spectrometer with homodyne detector. The microwave source emits the radiation, which goes through the sample to the detector. The table consists of the microwave components, microwave source, low oscillating (LO), reference and microwave detector. The sample is placed in the superconducting magnet.

Where the *energy dissipated per cycle* means the amount of energy lost during one microwave period. Energy can be lost in the form of heat on the side wall of the cavity because electrical current is generated by the microwaves in the side walls of the cavity. The  $Q$  factor [4] can be also measured and it is expressed as:

$$Q = \frac{\nu_{res}}{\Delta \nu} \quad (2.2)$$

Where  $\nu_{res}$  indicates the resonance frequency and  $\Delta \nu$  is the bandwidth.

Standing waves occur as a consequence of the reflection of waves with integral

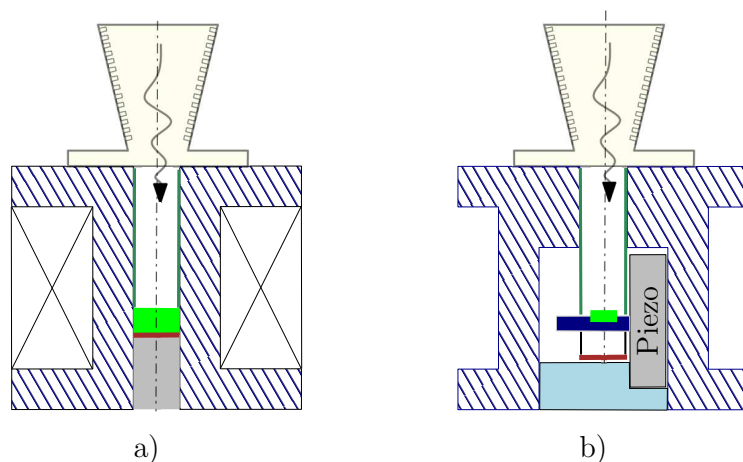


Figure 2.3: Scheme of commonly used sample holders attached to the corrugated taper. a) Non-Resonant cavity is an ordinary holder which can be used for many types of samples, b) the rotating sample holder with the piezoelectric rotator.

multiples of resonance frequency. Standing electromagnetic waves are composed by the electric and magnetic field components. In the place where the electrical field is maximum, the magnetic field is minimum and vice versa. Many samples have non-resonance absorption of the microwaves through the electric field and the  $Q$  factor can be diminished by an increase in dissipated energy [4].<sup>1</sup> Nevertheless, in the EPR experiment, the interest is in the absorption of the microwave energy due to the incident oscillating magnetic field. Therefore, the biggest signals and the highest sensitivity is obtained, when the sample is placed in the position of maximum magnetic field and minimum electric field. [1].

The cavities are designed for optimal placement of the sample. The typical samples are in the liquid or solid state and can be as a powder in form of mould cylindrical tablets or single crystals [22]. Underneath the sample is often placed a mirror, which reflects the microwave radiation, but it depends on the mode of the measurement.

The dimensions of sample holders are limited by the magnet gap, where the holders are inserted. Types of sample holders are depicted in Figure 2.3.

### 2.3.1 non-resonance Sample Holder

Non-resonant sample holder is commonly used in HF-EPR spectroscopy and it is distinguished by simpleness of utilize. The main advantage of non-resonance sample holders lies in its capability to work in a wide range of frequencies [24]. Hence, it is

<sup>1</sup>The microwave oven is based on this principle.

the most common choice for sample holders in broadband multi-frequency studies. Another advantage is a simple handling and loading of the sample. Therefore, the non-resonant sample holders are used for an observation of powder, liquid and frozen specimens. Non-resonant sample holder is suitable for high loss samples such as thin films, or samples in which the losses are dominated by magnetic effects [22].

Non-resonance sample holder can be imagined as a piece of a cylindrical material and it holds the sample between two windows in the beam path of a transmission spectrometer [22]. This type of sample holder works with small reflected mirror, which is placed beneath the sample.

### **2.3.2 Rotating Sample Holder**

The rotating sample holder is distinguished by the possibility of rotation of the sample [22]. This is very useful for orientation studies of single crystals and for anisotropic samples.

The rotating sample holder consists of the main holder part, where the rotatory power unit is placed. The often used unit is a rotating piezoelectric nanopositioner with a resistive encoder because of its possibility of working in magnetic field surroundings. The propulsion of rotation motion can be either directly by the nanopositioner to rotating sample holder, or over a gear mechanism. The type of propulsion depends on space in the cryostat.

## **2.4 Magnet and Cryostat**

For creating homogeneous magnetic field up to several tesla, the electromagnet is applied. In case of HF-EPR spectrometer, the superconducting magnet is used because it can provide stronger magnetic field (usually up to 16 T) which is necessary because of the resonance condition [25]. Nevertheless, the superconducting magnet must work at cryogenic temperatures during its operation. The extreme low temperature is achieved by the liquid (pumped) helium and the liquid nitrogen is used in system to help isolate the helium chamber from the higher temperature of the external environment [26]. The magnet is placed in the cryostat, where these conditions are established. Cryostat, which makes possible measurement at different temperatures, is very useful. Thanks to variable temperature in cryostat, temperature sensitive samples can be measured and afterwards their spectrums can be compared. The temperature range of cryostat is from 1.5 to 300 K because of the variable environment for measured sample. The superconducting magnet is shown in Figure 5.1.

## 2.5 Detector

The main role of the detection system deals with the measurement of the microwave energy which is absorbed by the sample. For detecting EPR signal a homodyne or a superheterodyne detectors can be used [14]. In the homodyne detector, the microwave radiation is firstly divided into reference and irradiation arms. Then both radiations are mixed again into homodyne detector. For the homodyne detection the bolometer can be applied due to possibility of using broad range of microwave frequencies. Therefore, the measurement with different frequencies can be performed by one detector.

The superheterodyne detections uses one source for creating the local (reference) frequency  $f_{LO}$  and the second source for the excitation  $f_{ex}$ . Shortly afterwards, these frequencies with a small difference of microwave energy are mixed into the detector, where the intermediate frequency  $f_{IF}$  occurs. Intermediate frequency is subsequently applied for creating spectral lines. The heterodyne detector, used in pulsed EPR, works only on fixed microwave frequencies. Advantage of heterodyne detector lies in very fast respose of signal [14].

For better detection of the signal, the modulation coil is applied. It produces a small oscillating magnetic field which is surrounded by the main magnetic field. Composing of frequencies of small modulated and main magnetic field is called lock-in technique and it is almost always used for amplification of the signal. Improved signal is affected by suitable choice of frequencies [12]. The amplifying spectrum is shown in the Figure 2.4.

## 2.6 Computer Controler

The EPR spectrometers are commonly equipped by the computer with suitable software which allows to drive experiments. The software, often home-built, depends on requirements of measurement.

The next chapter will deals with the basics of Gaussian Beam Propagation.

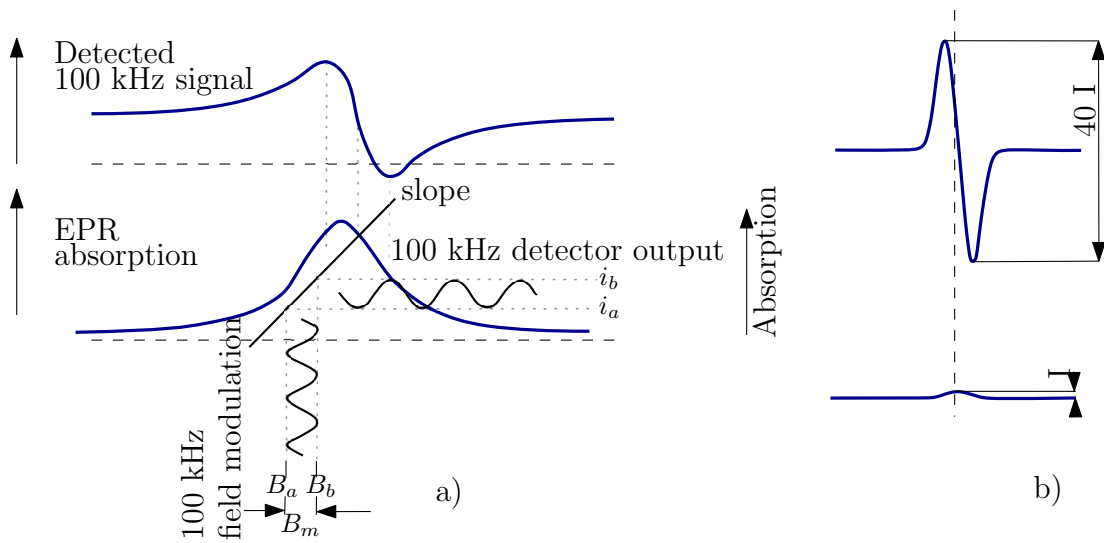


Figure 2.4: Schematic description of effect of small-amplitude field modulation on the detector output current. The static magnetic field is modulated in range of the restrictions  $B_a$  and  $B_b$ . Not to scale, taken from [1]. (b) Simulated effect of field modulation regarding intensity enhancement. It indicates the difference between minimum and maximum value of absorption intensity. The same value for a modulated signal can be almost forty times higher, depending on modulation amplitude and the linewidth. Taken from [27].



### 3 QUASIOPTICS

Quasioptics (QO) is a discipline of the propagation of electromagnetic radiation and it deals with the microwaves of the wavelength between ray and diffraction optics. Ray optics engages in the radiation when that wavelength  $\lambda \rightarrow \infty$  and the dimensions of all components such as lenses, mirrors and apertures compared to the wavelength dimension, are negligible. The diffraction optics operate with wavelength limit  $\lambda \approx \textit{system dimensions}$  and their utilize is relatively difficult and time consuming in comparasion with use of ray optics. The nature of the QO system is appealingly described by a theory of Gaussian beams propagation [16].

The QO components were primarily developed for an astronomy-related research. Due to low-loss propagation of the signal, this approach became very important in radio communication in astronomy. Low losses allow moving up the boundary of the frequency range [28].

There are several advantages of using QO in EPR spectroscopy. The low-loss propagation of the microwave radiation can be considered as the first one. The next one lies in possibility of same geometrical parameters of components. Furthermore, the QO components can be proposed for a wide frequency range. For this reason, the multi-frequency EPR spectrometers are used. Nowadays, thanks to its advantage, QO have become an integral part of most EPR spectrometers [29], [30], [31].

The main task of this chapter is to introduce the basic theory of the Gaussian beam propagation of millimetre and submillimetre waves and its application in EPR [16].

#### 3.1 Gaussian Beam

For the description of an optical system, it is appropriated to use Gaussian beams which are coherent during its propagation. The coherent beam has low divergence and the same phase difference [16]. This phenomenon happens when the system dimensions, such as lenses, mirrors, propagation distance are larger than the beam wavelength and when the direction of propagation is parallel to the optical axis. This occurs when the beam stays well collimated and the diffraction effects are restricted.

A mathematical description of Gaussian beams proceed from two presumptions. Firstly, when the deviation of the beam amplitude of the wavefront and the wavelength are compared, the new incurred distance is small. Secondly, this deviation should then be smaller than the deviation perpendicular to the propagation axis [16].

The fundamental Gaussian beam is described by the equations:

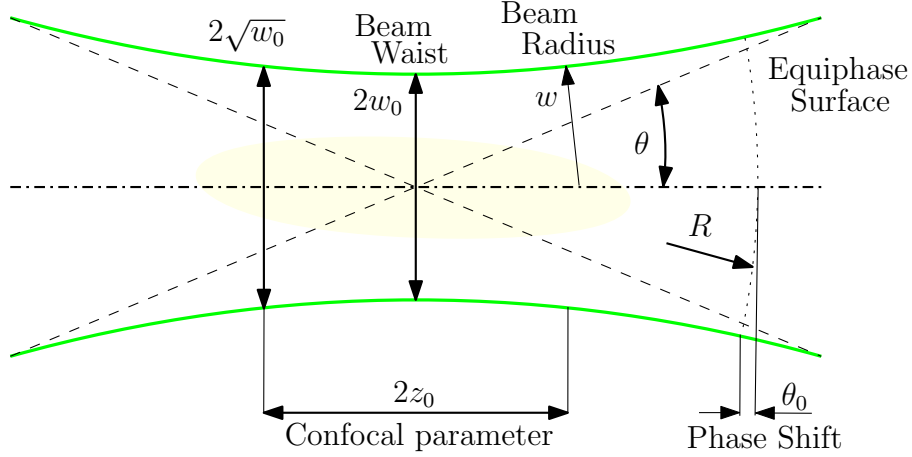


Figure 3.1: Schema of Gaussian Beam. Taken from [16]

$$R = z + \frac{1}{z} \left( \frac{\pi \omega_0^2}{\lambda} \right)^2, \quad (3.1)$$

$$\omega = \omega_0 \sqrt{1 + \left( \frac{z\lambda}{\pi \omega_0^2} \right)^2}, \quad (3.2)$$

$$\tan \theta_0 = \frac{z\lambda}{\pi \omega_0^2}, \quad (3.3)$$

where  $R$  designates the wave front radius,  $\omega$  is the radius in which the electrical field  $E$  falls to  $1/e$  relative to its axial (maximum) value for the  $z$  position. The beam radius is called  $\omega$  and  $\theta_0$  designates the Gaussian beam phase shift. Beam waist radius, or simply the beam waist, is designated by  $\omega_0$  and it occurs in each equation. The beam waist  $\omega_0$  characterizes also the position  $z = 0$  and designates the minimal size of the beam radius  $\omega$ . All of these parameters are shown in Figure 3.2.

## 3.2 Inverse Formulas for the Gaussian Beam

The inverse formulas, calculated backwards, are needed for determination of the unknown parameters of the beam. Because in practice, the size of the Gaussian beam  $\omega$  is only known from measurements. Moreover, this beam is generated by a conical horn at a specific position  $z$ . The inverse formula of the beam waist  $\omega_0$  and its location  $z$  are:

$$\omega_0 = \frac{\omega}{\sqrt{\left(1 + \left(\frac{\pi\omega^2}{R\lambda}\right)^2\right)}}, \quad (3.4)$$

$$z = \frac{R}{1 + \left(\frac{R\lambda}{\pi\omega^2}\right)^2}, \quad (3.5)$$

it is necessary to know the position  $z$  and the microwave beam waist  $\omega_0$  because of the accurate subsequent coupling of conical horn to the sample holder.

The optimal Gaussian beam radius  $\omega$  in the aperture  $a$  is shown by the equation 3.6. The aperture  $a$  and circular corrugated waveguide (conical horn) will be optimally coupled to the surroundings system.

$$\omega = 0,644a \quad (3.6)$$

for other kinds of waveguides, an accurate equation can be found in the book of Goldsmith [16].

### 3.3 Confocal Distance

The term confocal distance  $z_c$ , also called the Rayleigh range or simply the depth of focus, represents a main role in optimizing the system. It is defined as:

$$z_c = \frac{\pi^2}{\omega_0} \lambda \quad (3.7)$$

two cases of confocal distance, which are influenced by different conditions, can be noticed. The first one, the near field region has the condition  $z \ll z_c$  whereas the condition of another one is:  $z \gg z_c$ .

### 3.4 Beam Coupling

A very important factor during designing the QO components is the correct beam coupling. Because even the slightest deviation causes losses of the propagated beam power.

The coupling efficiency can be defined as a ratio of the power gained by a detector to the power emitted from the source. When all QO components are accurately aligned, the ratio equals one and the losses are negligible. Inappropriate beam coupling can also cause creating of undesirable waves.

In HF-EPR, even very small misalignment of coupled QO components, which causes the microwave power losses, can be significant. Therefore, the QO waveguides

have to be sufficient robust and created with precision of the order of tenths of millimeter. The three simplest misalignment types are shown in Figure 3.2.

The following chapter will deal with the requirements and constructional techniques and with the design of components placed in extreme conditions.

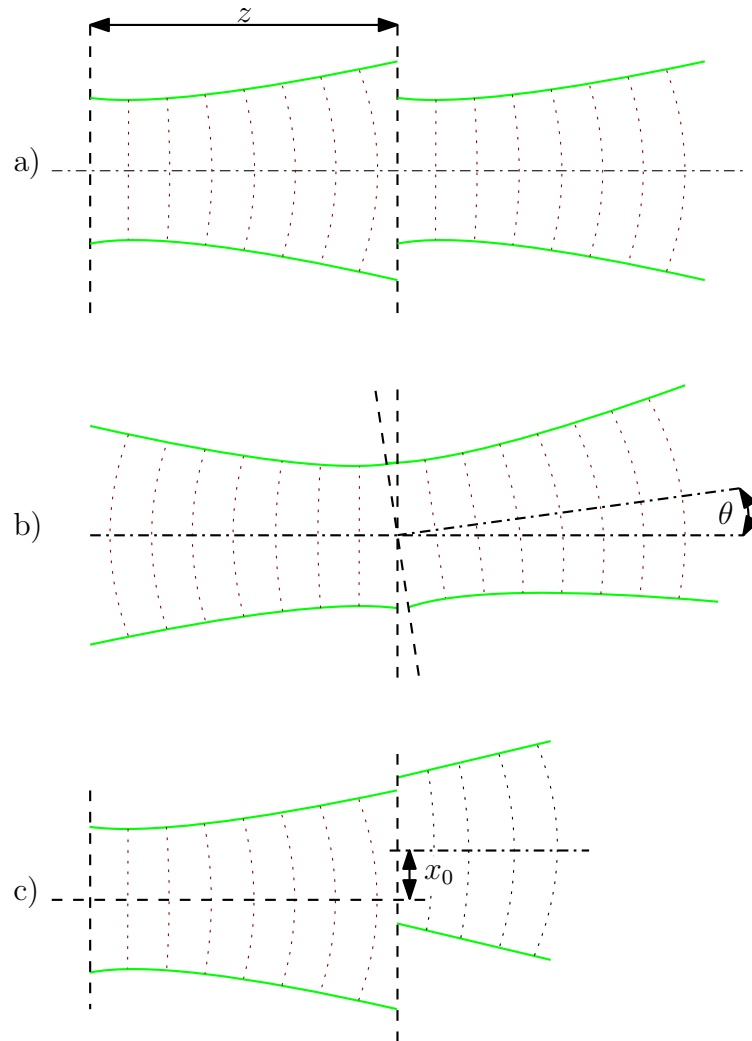


Figure 3.2: Three general cases of Gaussian beam misalignment. (a) Axially aligned beams with offset waist  $\Delta z$ , (b) titled beams with angle  $\alpha$  (c) radially offset beams of  $x_0$ . Taken from [16].



## 4 REQUIREMENTS AND CONSTRUCTIONAL TECHNIQUES

The main task of this practical chapter lies in the proposal of the design of sample holders working with specific conditions. Therefore, there are several restrictions. The sample holders are exposed to the temperature range between 1,8 to 300 K, to differences of pressures and to very strong magnetic field up to 16 T. Furthermore, the most important restriction is that the outer diameter of the sample holder is limited by the input size of insert (50 mm in diameter). The restrictions are not easy to adhere. For this reason, the proposal of sample holder requires distinctive process and use of fundamental rules mentioned below.

### 4.1 Construction at Low Temperatures

The following section is aimed to describe details of sample holder construction. The technical requirements of the system and the outline of their solutions are mentioned in next paragraphs.

#### 4.1.1 Requirements for Sample Holder Design in Low Vacuum Environment

The advantage of designed sample holders is the possibility of implementation in the environment of low pressure. The low vacuum inside the magnet is created because with the decreased pressure, the temperature also diminished. This environment brings considerable limitations in design of sample holders, especially regarding usable materials. Only a certain number of materials fulfils required conditions. This group of usable is further limited with different types of vacuum [32]. Furthermore, some special materials necessitate particular machining process. The sample holder of HF-EPR spectrometer will be designed to work in low vacuum ( $10^2$  to  $10^{-3}$  Pa) [33].

#### 4.1.2 Desorption of Gasses

Supposing the vacuum chamber is totally sealed, the pressure in this chamber can be expressed by the equation:

$$p = \frac{QA}{S} \quad (4.1)$$

Where  $S$  is the pumping pace of vacuum system,  $A$  designates the whole area of the surface inside the chamber and  $Q$  is the coefficient of desorption of gasses (filling) in

the chamber [34]. The pressure is therefore dependent on the spontaneous release of particles (such as release from the surface) when the vacuum environment is set up. For this reason, the choice of suitable material is fundamental for the construction of vacuum-compatible devices. The main requirement is low desorption value relative to the area unit. Selected materials should also be as clean as possible with a small amount of internally bound gases. Both of these requirements considerably affect the time of creating the vacuum chamber.

Stabilization of vacuum can be also affected by the presence of water. Water is easily attached to almost all materials. In form of a thin layer on the surfaces, which is removed by blowing the vacuum chamber at temperatures of 420 – 480 K. Therefore, the temperature stability of the material is important and the desorption of gases from the used materials should not exceed the allowed limit.

### 4.1.3 Leakage

One of the biggest problems in achieving the desired vacuum is leakage. If the leaks are too large, the required pressure must be stabilized in the cavity. Moreover, the system can be also affected by small leaks. In this case, sample contamination and degradation of measurement results may occur.

Leaks can be divided into external and internal. The external ones can be caused by the chamber itself, for example, by poor welding of the chamber, possibly by mechanically movable joints [35].

Internal leaks are mainly caused by mechanical machining. These are, for example, virtual leaks caused by the release of gases from cracks, by a porous material or inappropriately utilize constructive design. For example, the virtual leaks can occur in place of a tight bolt. The example of virtual leak can be seen in Figure 4.1. The solution to this problem lies in the chamfering of one side of the bolt, drilling the hole through the screw or laterally boring the hole into the material with thread. Internal leaks can also occur due to the unsuitable type of welding or soldering.

### 4.1.4 Mechanical Connections

All mechanical components used in the vacuum chamber has to yield to stringent criteria to reduce the amount of desorption of gases. For this reason, the correct procedure for creating mechanical joints is essential. It is fundamental to avoid use of fasteners with additives which pollute the chamber [36].

Welded joints are classified as non-detachable joints, which in inappropriate design, can create cavities and significantly affect the formation of vacuum. The solution to this problem is the welding of materials directly in the vacuum, for example



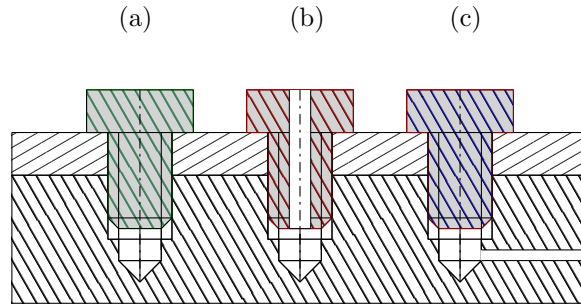


Figure 4.1: The case including the cavity a), the possibilities to avoid the closed cavities b) drilling a hole through the screw in axis direction c) drilling the hole to the cavity from side. Taken from [37].

by electron beam or in a protective atmosphere of inert gas.

At the earliest, welded materials should be thoroughly cleaned and exhausted. A suitable type of weld is a butt weld whose quality can be checked throughout length. It is necessary to use welds (as fillet weld) with caution because they can cause obstacles for formation of the vacuum. Types of welds are shown in Figure 4.2.

Acceptable welds:

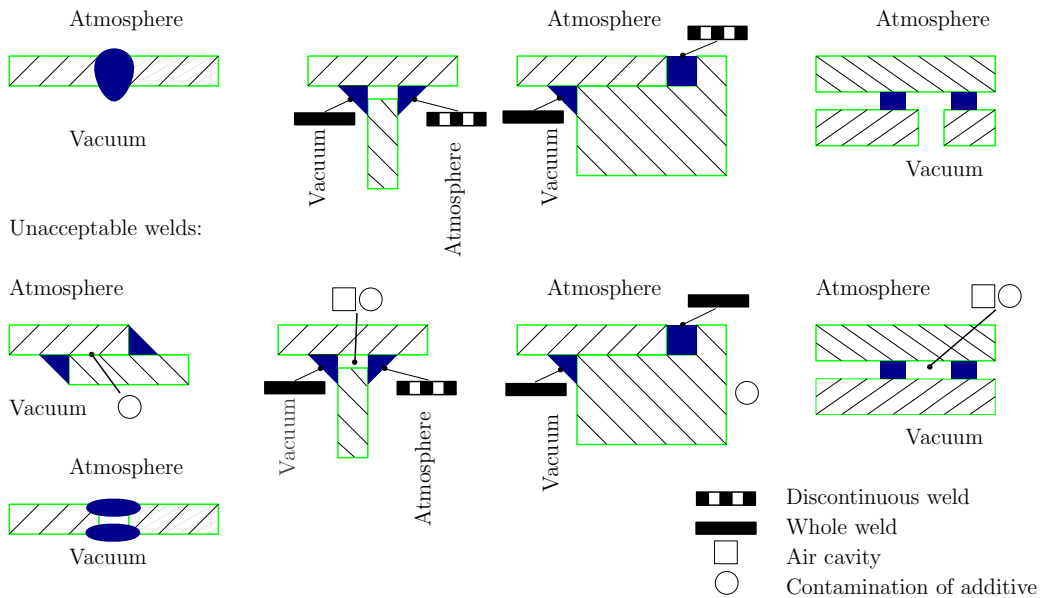


Figure 4.2: The cases of vacuum acceptable and unacceptable welds. Taken from [35].

The next commonly used type of connection is soldering. Thanks to this kind

of connection the joints are precise and tough. For soldering the soldering flux with different melting temperature is used. However, it is necessary to avoid soldering flux with low melting temperature for components, which are determined for a burning. Because the soldering flux can melt during burning and it can cause the disconnection of components. Burning is a method of removing water from the surface of components [35].

#### **4.1.5 Cleanliness of Components**

The cleanliness of components used at low temperature and pressure is very important for a formation of the vacuum chamber. For example, residual oil and lubricants with low saturation vapor pressure (ex after machining) have to be removed otherwise they can cause pollution and increase pump time. The suitable process should be chosen for diverse materials which are often cleaned in different ways.

For all materials, the surface quality of components is substantial because of gas adsorption and desorption. The surface should be smooth, without cracks and pores. For processing and obtaining the desired surface quality, shaving, mechanical or electrochemical polishing is applied.

## **4.2 Selection of Materials for Cryogenic Environment**

The choice of desirable materials (table 4.1) plays a major role in the proposal of EPR. By understanding of basic material properties, the requirements such as thermal and mechanical stability, electrical and thermal conductivity, low porosity and a small amount of microcracks, microwaves reflectivity can be achieved.

The thermal stability gains importance over a connection of two different materials because of a thermal expansion. The thermal expansion represents a phenomenon, when the dimensions of solid are changed depending on temperature. Therefore, materials have the coefficient of thermal expansion. The thermal stability can be utilized for rigid connection of two materials, which have the different coefficient of thermal expansion. On the other hand, for a moveable and accuracy connections, the thermal expansion of two different materials as low as possible is required.

The thermal conductivity of materials is important for the reason of transmission of heat. The thermal conductivity has to be considered for all parts, where the temperature is changed. For example in EPR spectrometer, the probe leads the

Table 4.1: Selection of commonly used materials in EPR spectroscopy. The thermal properties are also shown. Taken from [38], [39], [40], [41], [42].

		Thermal capacity	Thermal conductivity
		[J/gK]	[W/mK] (at 273 K)
Metals	Stainless Steel	0,460	12,0
	German Silver	0,394	24,9
	Gold	0,128	319,0
	Brass	0,820	106,0
	Copper	0,379	403,0
	Titanium	0,511	22,0
	Aluminum	0,880	38,0
Polymers	PEEK	0,580	0,3
	Vespel	1,130	0,4
	Teflon	0,960	0,2
Others	Sapphire	0,761	23,1
	Quartz	0,730	11,0
	Silica	0,710	1,6

heat inside the cryostat because the first part is situated in the environment with the room temperature and the second part is placed into cryostat with low temperature.

The heat capacity closely relates to the thermal conductivity and it constitutes the amount of energy necessary to increase the temperature of a known quantity of a system on the degree [43]. Hence, the heat capacity is necessary to consider for parts, where fast cooling is required.

The main requirement of the design of sample holder deals with the choice of materials, which have to be non-magnetic because all proposed components are placed in the middle to the superconducting magnet. For EPR spectroscopy, several materials are employed, which are shown in table 5.1, where they are divided into different groups.

An essential part of the material selection is also its price, which is usually higher than the price of conventionally used materials. For this reason, it is suitable to consider the shape of the part and reduce the losses of material caused by the machining.

All these mentioned knowledge will be utilized during the proposal of EPR components which is described in the next chapters.



## 5 MULTI PROPOSE HF-EPR SAMPLE HOLDER

The following two chapters deal with the new design of sample holder. All 3D models of components were created in PTC Creo 4.0 [44]. Both sample holders were developed at CEITEC – Central European Institute of Technology in Brno [45].

### 5.1 The Probe

The probe, depicted in Figure 5.1, is a name of part, which carries and partially covers all components placed in the cryostat. It constitutes a boundary between the room and cryogenic environment because the part of the probe is placed inside the cryostat and the second part is placed out of the it. The probe is consisted of a head, the microwave waveguide, the sample holder, the heat shields and a cover of probe. The environment inside the probe is filled by Helium because of better cooling of the sample in cryostat. From this reason, the probe has to be hermetically closed.

The head of probe is situated in the room environment on top of the cryostat and it consists of a housing head, feedthroughs, components for connection of the microwave waveguide and the insert of covered pipe. The microwave waveguide is connected to the head of probe by three screws and a flange in shape of a triangle for the reason of place saving inside the probe. The beginning of the waveguide is covered by a Teflon plate, which allows the microwave radiation penetrate through it very well. The Teflon plate has to contain a special coating which prevents the creating of standing waves [46]. This fact is caused by Brewster's angle [47] when the beam of microwave radiation is perfectly transmitted through dielectric surface without reflection. The Brewster's angle is defined by following equation:

$$\tan(\theta_B) = \frac{n_2}{n_1} \quad (5.1)$$

where  $n_1$  indicates the refractive index of original environment  $n_2$  is the refractive index of the environment into which the beam is coming [43]. In case of spectrometer, the microwave beam is coming from the air ( $n_1 = 1$ ) to the Teflon ( $n_2 = 1,71$ ). The Brewster's angle, in this case, is equal to  $\theta_B = 59,7^\circ$  and it is depicted in Figure 5.1.

The feedthroughs are placed on the sides of the head and they are used because of the different environment between cryostat and the room. They connect the wires and optical fiber. The connection between the head of probe and the covered pipe is performed by welding. The microwave waveguide with corrugations goes through the head to the sample holder. The microwave waveguide and the head of probe are

developed by Thomas Keating Ltd. [48] company, which is also responsible for their manufacturing.

To avoid the contamination of Helium by other gas, the probe is covered by the thin-walled pipe. The pipe consisted of two welded parts, is inserted into the head of the probe. The upper part of the pipe is made of nonmagnetic stainless steel because it transfers less heat. The lower part of the covered pipe is made of brass due to better transferring of heat between the environment out of the magnet and of the sample holder. The part of pipe made of brass is ended by the circular brass plate which is welded to the pipe.

Inside the covered pipe, the heat shields are regularly placed. They create separated smaller chambers inside the probe which reduce transferring of heat between the head of probe and the sample holder. The heat shields are directly connected by soldering to the microwave waveguide. The total number of used heat shields is five and they have drilled holes for propelled axis and small pipes (see section Propulsion of Carousel 6.1.2). It is necessary to ensure the alignment of holes because the misalignment could cause worse transfer of torque for the propulsion of the carousel.

Because of many wires, which have to be led to the sample holder, the thin-walled pipes are employed. They go through the all heat shields and constitute the easy way for wiring.

## **5.2 Connection of Sample Holder and Corrugated Taper - Locking System**

The first task of the thesis was to solve the connection between the sample holder and corrugated taper, simply to create kind of locking system. Nowadays, the connection of these parts is commonly performed by bolts or threaded flanges. The connection should be as fast as possible because some cooled samples are put inside the holder and long time of connection could cause heat changes. Also, the connection of these parts should be easy to handle and it should be compatible with the other kinds of measurement, such as Far Infrared. The connection or disconnection of both parts is carried out at the room temperature and whole assembly is subsequently placed into the cryostat. From these reasons, several proposals of locking system were created, two of them are depicted in Figure 5.2.

The first proposal deals with utilize of click system (Figure 5.2 a)). Two detents on sides are pushed by prestressed springs inwards which prevent the spontaneous becoming loose. Therefore, the sample holder is connected to the corrugated taper with the simple click from the bottom side. Disassembly of these both parts is performed by tilting of detents and removing of the sample holder from the flange

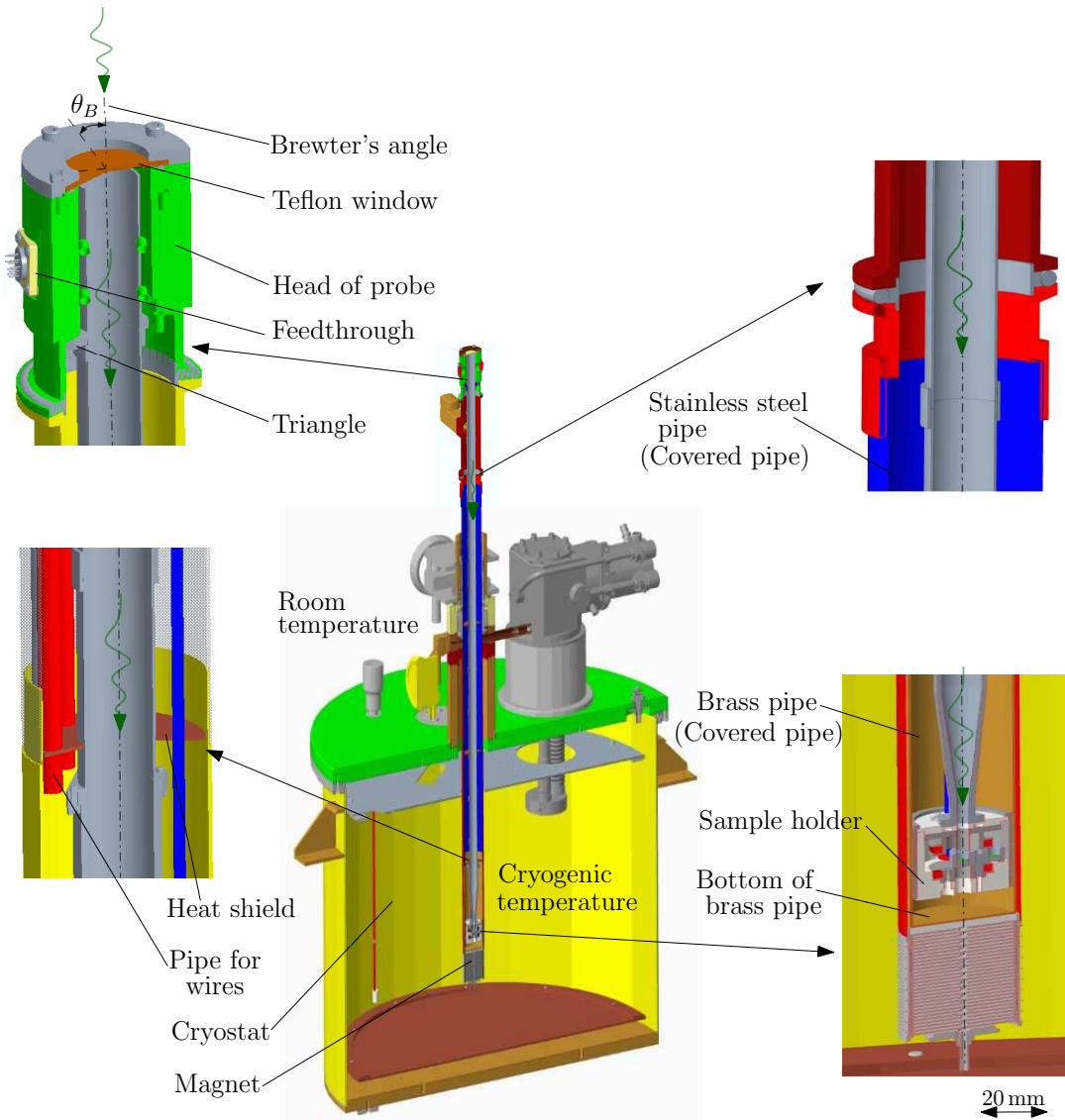


Figure 5.1: The superconducting magnet placed in the cryostat. The head of probe is placed at the room temperature out of the magnet and is inserted through the hole in the cryostat with low temperature inwards. The main parts of the probe are briefly shown in sides of the figure.

of the corrugated taper. However, there are several complications. The main one deals with the tight connection. After ensuring of detents at the connected position, even small clearance causes the loose connection. It has undesirable influence for misalignment of connected components and it leads to losses of the microwave (see section Beam Coupling 3.4). The size of the space, where the sample holder is situated, represents next complication. During the remove of the sample holder, the detents have to be tilted away. But the sample holder is placed in the thin-walled

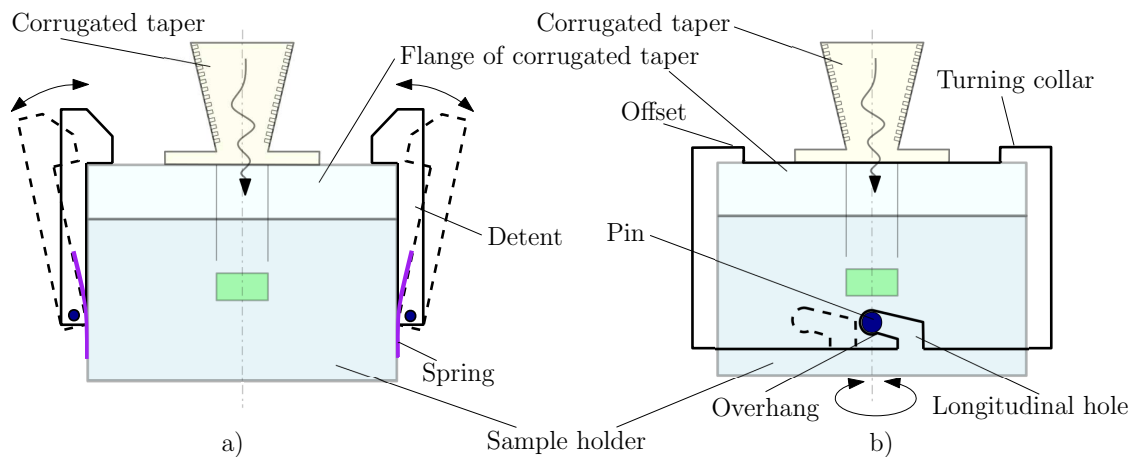


Figure 5.2: The schema of connection between sample holder and corrugated taper - locking system. a) it is the connection with use of detents, b) the collar ensures the tight and right connection. The unlocked system is depicted in Figure 5.3.

pipe with outer diameter 50 mm and there is no space for this motion.

Therefore, the next proposal was suggested. The connection of the sample holder and corrugated taper uses a turning collar (Figure 5.2 b)). The motion of collar is limited by its offset at the section of corrugated taper. The sample holder is connected by four pins, which can easily slide in longitudinal holes depicted in Figure 5.3. Due to rising shape of longitudinal holes, both parts are firmly tightened together and the creating of misalignments is negligible. Spontaneous disassembling of connected parts is prevented by small overhangs in longitudinal holes that secure rotating collar in the tightened position. Due to spontaneous disassembling, the turning collar with threads was not suggested. To remove the sample holder from the corrugated taper, it is necessary to turn the collar in reverse direction and take sample holder down. The advantage of connection by rotating collar lies in tight and fast connection.

### 5.2.1 The Flange of Corrugated Taper and Sample Holder

The next requirement lies in an implementation of a general purpose flange of corrugated taper, which can be applied for various types of the sample holders, such as the rotating sample holder or non-resonance sample holder. Each sample holders must have its own flange. Therefore, the main task of flange of corrugated taper deals with the support for the locking system and for connected parts, such as the connectors of wires, or the propelled shaft.

Into the sample holder, essential types of wires are led. Their main task is to



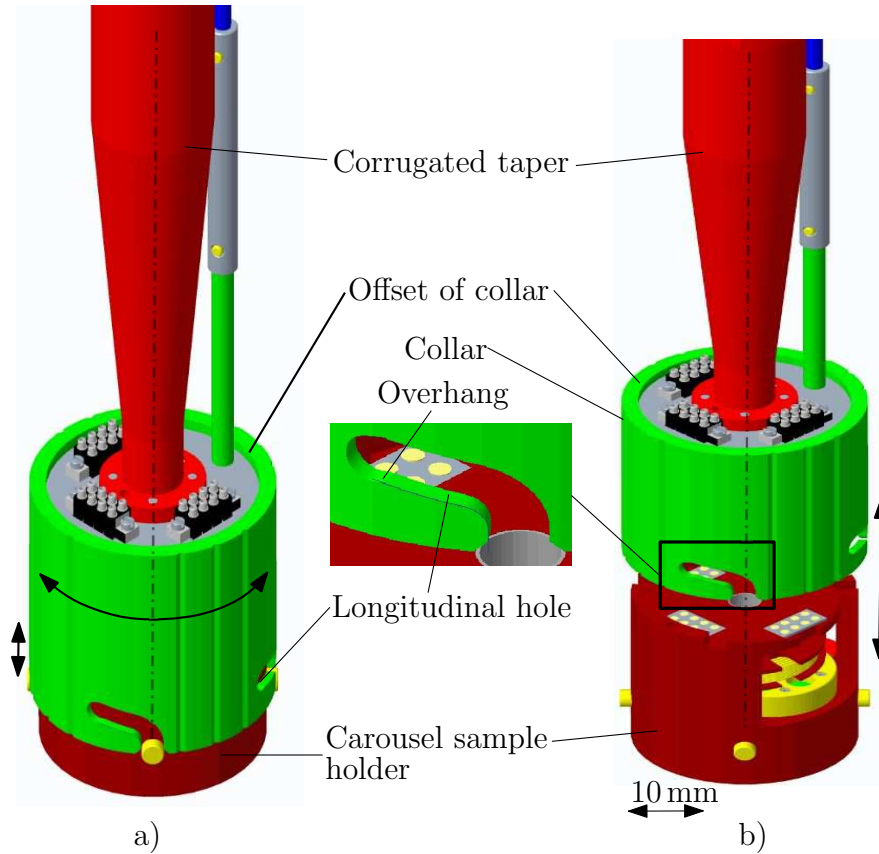


Figure 5.3: The locking system is ensured by the collar, which has the longitudinal rising hole. The spontaneous disassembling of connected parts is prevented by small overhang. The sample holder is taken out downward. The situation a) signifies realizing of connected parts, b) the sample holder can be taken out.

control sensors, piezoelectric rotator, modulation coil and etc. Nevertheless, because of using locking system, the wires have to be firstly split and then during attachment of the corrugated taper and the sample holder connected again. Therefore, the connectors of wires, which are placed inside the special removable flange of corrugated taper (Figure 5.4), are applied. The total number of the needed led wires is 24 (three wires for temperature sensors, 14 wires for bolometers, two wires for modulation coil and five for piezoelectric rotator).

For carousel sample holder (described in the following section), the propelled axes, which has to be connected at the place of two flanges, is employed. The connection of propelled axes, depicted in Figure 5.4, is performed by chamfer at one of the ends of both axes. It is described in the subsection Propulsion of Carousel 6.1.2.

The flange is connected to the corrugated taper by four screws and its shape is

designed with regard to alignment. Alignment is ensured by recess placed close to the outer circumference of the flange which is inserted into the opposite part of the sample holder. The shape reflects the requirement of mistake-proofing<sup>1</sup>, therefore there is drilled one hole for a pin with only one possibility of the connection.

It may seem that the flange as separated part does not have to be used because it could be directly replaced by corrugated taper with the flange of big diameter. Nevertheless, the taper is made by the electroforming method and the growth of material of bigger size is too expensive and time consuming. Therefore, the taper is made on the suitable diameter ( $\phi 30$  mm) and then it is connected to the flange.

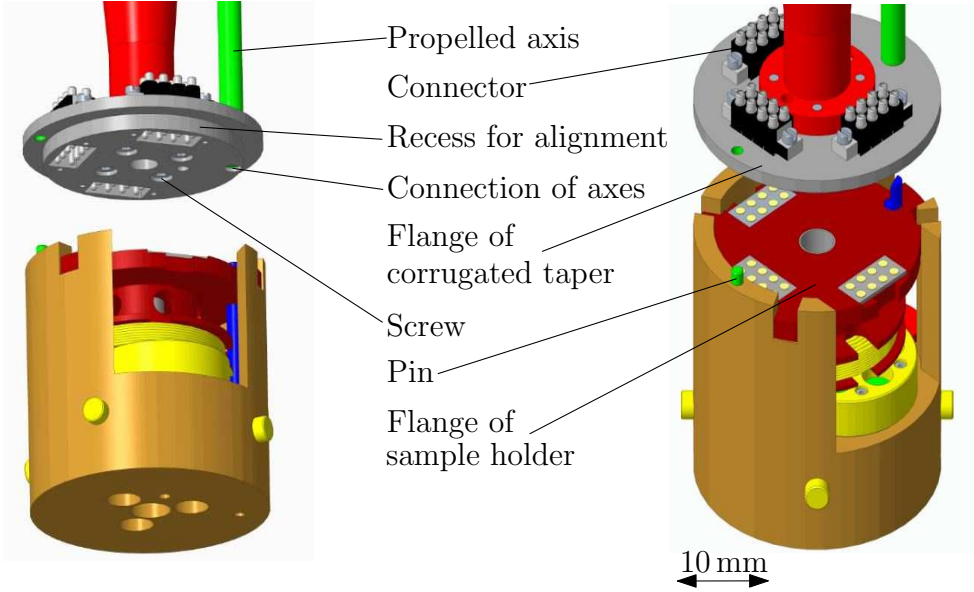


Figure 5.4: The flange of corrugated taper and sample holder.

This chapter was dedicated to the proposal of the probe and connection between microwave waveguides and sample holder. In the next chapter, the current solution of sample holder design will be explained.

---

<sup>1</sup>The fail-safing (*Poka – yoke*) deals with the only one possible way to connect two components. By this, the risk of an unintentional mistake is minimized.

## 6 DESIGN OF SAMPLE HOLDERS

This chapter is divided into two parts. The first deals with the newly proposed design of carousel sample holder. The main task of next part lies in the proposal of new rotating sample holder. For manufacturing of both types, the 3D printing is proposed. The 3D printing allows production of components of nonmagnetic materials, such as stainless steel, titan or aluminum.

### 6.1 Carousel Sample Holder

Everything started with an idea of use of carousel. Currently applied sample holders carry only one experimental sample. Because newly proposed superconducting magnet for HF-EPR spectrometer allows using bigger type of sample holder, for this reason it is also possible that the sample holder can carry more than one experimental sample.

The motivation of design of carousel sample holder lies in its many advantages. For subsequent comparison of background spectra, the referent sample, which is placed into the carousel between other samples, can be used. Experimental samples can be also measured within almost identical conditions and they can be arbitrarily changed for later checking observation during the measurement.

Thanks to carousel sample holder, energy-saving is achieved. The first reason of energy-saving occurs because the superconducting magnet works shorter time. The next one is that the sample holder does not have to be cooled from the room to the low temperature during each sample exchange. The sample holder is cooled only at the beginning of the measurement and then it works at the similar temperature. The theoretical savings of energy are six times smaller than in case of conventional EPR sample holder.

The biggest benefit of carousel sample holder lies in time-savings. Commonly used HF-EPR spectrometers can measure only one sample as it was mentioned. For observation another sample, it is necessary to perform several acts, such as take out the probe from magnet, change of the sample itself, cooling of the sample holder, stabilization of environment inside the magnet and the measurement of the sample. The total time of changing of sample, measurement and the replacement of new sample usually takes ten hours. Thus, it takes sixty hours to measure six samples. By using carousel sample holder for six samples, the number of these acts is dramatically reduced. The cooling of the superconducting magnet, stabilization of environment inside the magnet and replacements of the samples fall off. Due to the complexity of the mass carousel sample holder, it is only necessary to stabilize the environment for longer period of time because of the bigger heat exchanges.

This approximated time of stabilization of the environment is increased by roughly five hours. But it suffices to do this movement only one time at the beginning of whole measurement. Therefore, the total estimated time for the measurement of six samples is 29 hours. So the total time-saving with utilize of carousel sample holder is more than fifty percent.

Last but not least, the measurement with the carousel sample holder is much more comfortable and pleasant for an operator of the HF-EPR spectrometer. It is, therefore, an automatization of the process. The less frequent changing of the sample constitutes the lower physical demands of the operator.

In HF-EPR spectroscopy, use of the carousel sample holder is very unique and it brings many advantages which are mentioned above.

This chapter deals with the description of proposal of carousel sample holder. However, there are several complications which are necessary to solve and optimize which are described in detail in following sections.

### 6.1.1 Selection of Mechanism

For changing of samples is necessary to use a mechanism which ensures the moving of sample. The sample changing can be performed by rotating, sliding motion or combination of both of them. It is necessary to set the samples into a central position which can be realized in several steps. Therefore, few proposals were suggested and two of them are depicted in Figure 6.1.

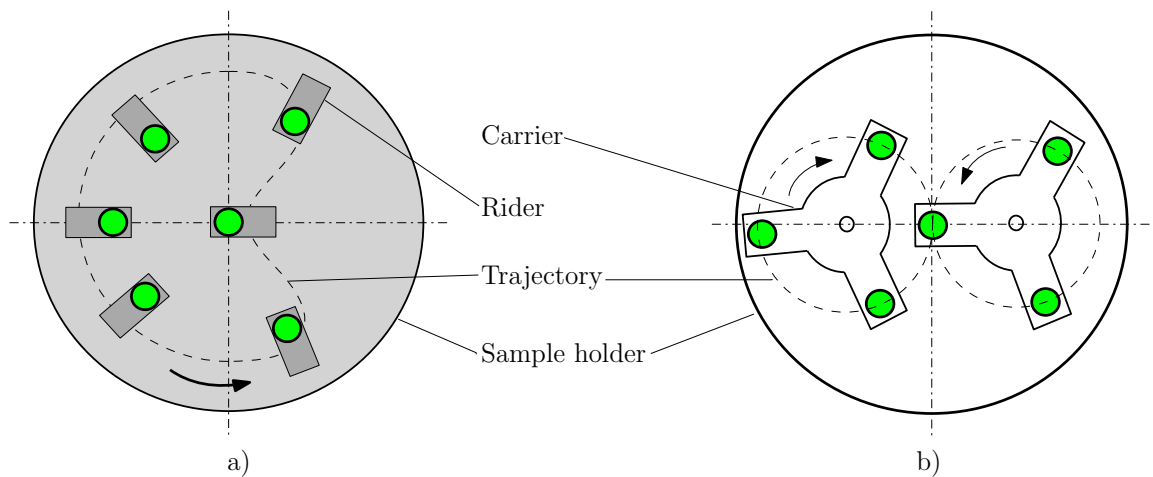


Figure 6.1: Possibilities of mechanism of carousel sample holder for six samples (green color). a) the mechanism with utilize of six riders, b) the mechanism with two rotary carriers for six samples.

The first case is based on the sliding motion on trajectory by the milled groove in the lower section of the sample holder (Figure 6.1 a)). The driver, which carries one sample, is moved by the propelled rotary carrier. The carrier, which allows the movement in the sample holder inward, has longitudinal holes. This kind of mechanism is very attractive, but overly complicated for use at low temperature because of many connected areas and complicated movement. There are seven moving units, six riders and one rotary carrier and the motion between each parts is largely sliding. For designing of devices used in cryogenic temperature, it is not able to use lubricants. However, in case of sliding motion, it is necessary to lubricate contact surfaces because the lubrication prevents creating abrasion. The solution to this problem could lie in use of Teflon material because it has great sliding property. But a thin layer of material would be peeled during sliding so this solution would be only temporary. Therefore, this mechanism was rejected.

Another proposal of mechanism deals with the use of two rotatory carriers Figure 6.2 b). They have arms in triplet shape and each arm carries one sample and the trajectory of samples is circular. The motion is ensured by gears which are placed beneath the carriers. Nevertheless, the problem occurs because of the dearth of space. Due to the inappropriate ratio between the width of the arm and the outer diameter of the carrier, the collision between arms of first and second carriers occurs. Even in case of designing different shapes of arms with recesses or rounded corners, it is not possible to avoid this undercutting. Moreover, this kind of mechanism uses three gears, which caused creating bigger clearance. So the use of the easier mechanism depicted in Figure 6.2 is desirable.

The final mechanism (Figure 6.2) is primary composed of rotary motion and of only two moveable components, such as the carousel and a pinion. Due to rotary motion of components, the friction between contacted areas is minimized. The advantage of this mechanism lies mainly in its simplicity. The carousel with the circular shape is situated on one side of sample holder housing, so the sample always goes through the center of the sample holder. For the propulsion of carousel, the gears are applied (see the subsection Gears 6.1.3). For the reason of distance saving between the sample and the Helmholtz coil (see the subsection Modulation coil 6.1.5), the tothing is directly cut on the perimeter of the carousel. Accordingly, the gear is not used.

## 6.1.2 Propulsion of Carousel

The propulsion of carousel, which is depicted in Figure 6.3, can be divided into two parts. The propulsive part works at the room temperature and it is placed out of the magnet. The propelled part is situated in the sample holder and it works at

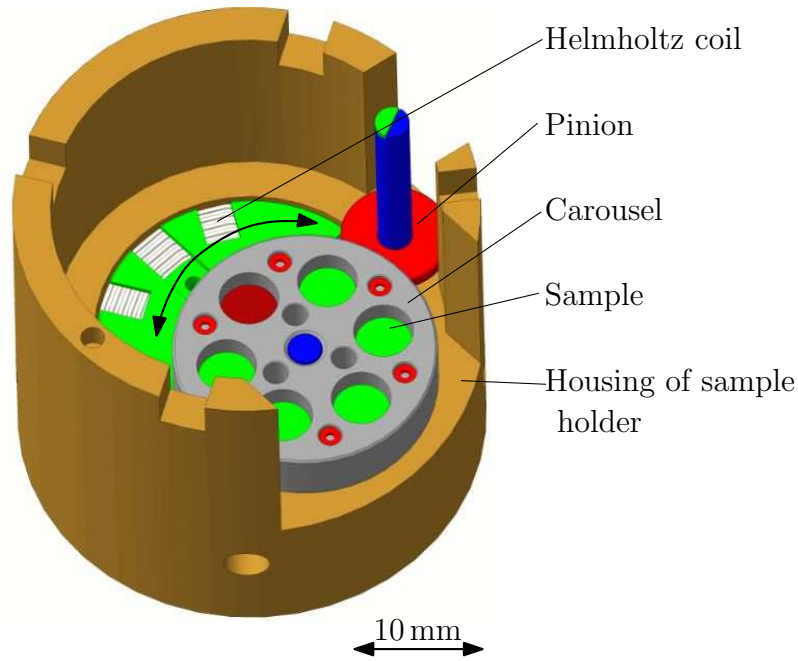


Figure 6.2: The mechanism of carousel sample holder for six samples.

cryogenic temperatures. Both parts are connected by the propelled axis which is divided into three parts. The whole propulsion system is shown in Figure 6.3.

The electric rotary stepper, type EMMS-ST 42 delivered by FESTO AG&Co.KG company [49], was chosen as the power unit. The stepper is placed on the support out of the head of probe. Because of the boundary between two different environments (one inside the probe and the another one of room temperature), it is necessary to seal the joint of rotary stepper and flange of head. Therefore, a sealing O-ring is used.

The torque continues through the horizontal axis to the perpendicular gears with frontal toothings, which is delivered also by the company FESTO AG&Co.KG. The axis is held by holder placed at the bottom of head of probe. The propelled axis is led to the flange of corrugated taper through the heat shields. A very important thing is that the drilled holes for the propelled axis in the heat shields have to be aligned. Otherwise, the resistance of rotary motion increases. Just above the flange of corrugated taper, the propelled axis is separated because of using of two corrugated tapers with different length. Various length is caused by different types of measurement. The connection of axis is performed by the clutch captured in Figure 6.3. The axis, which is coming into the clutch, has 3 mm in diameter and it is ensured by one pin. The axis, which is leaving the clutch downstairs, has 5 mm in diameter and it is also ensured by one pin but in two possibilities of height. For the reason of different temperature during assembling and working of the propelled system, the

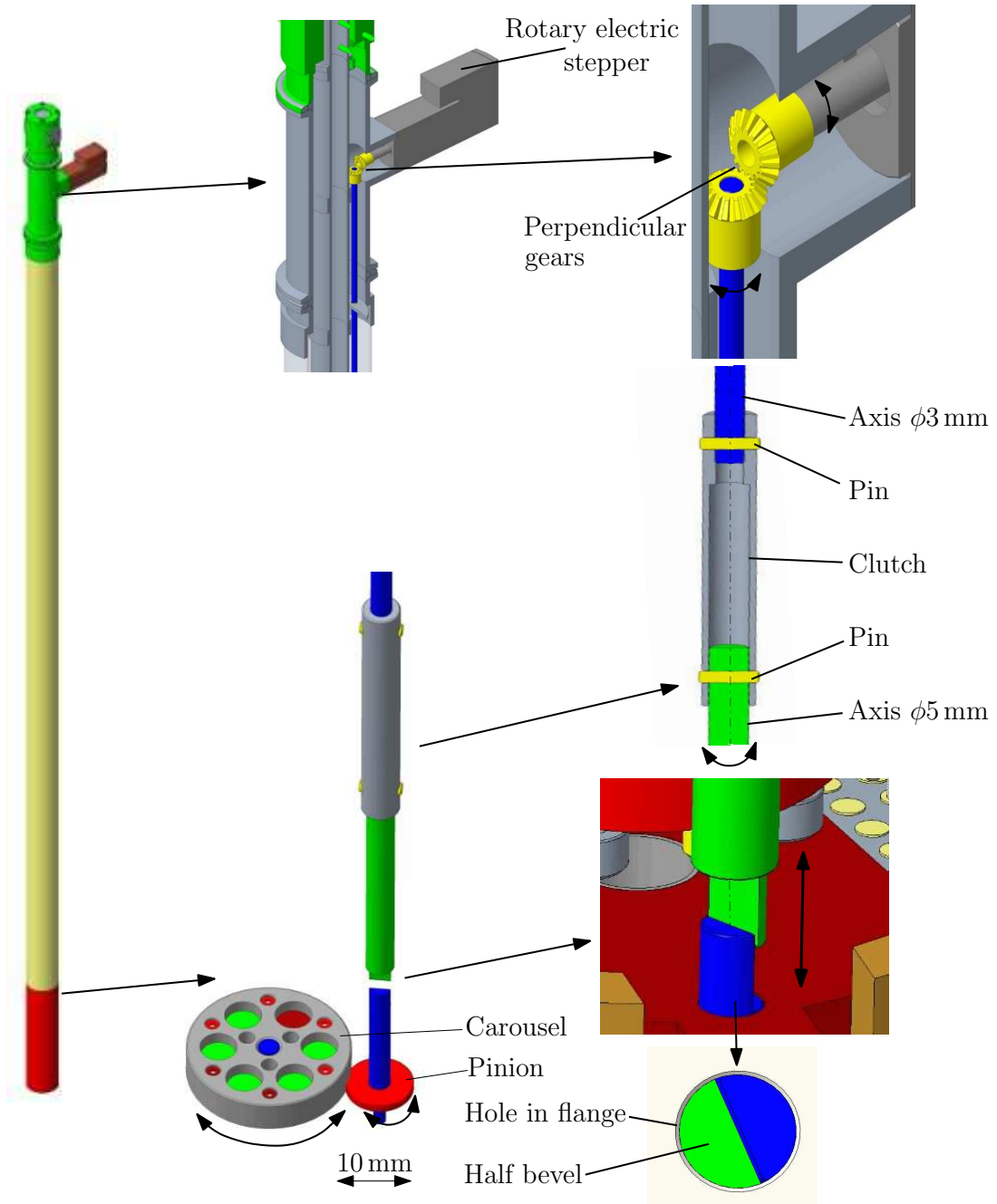


Figure 6.3: The propulsion of the carousel. The torque is led by the propelled axis to the carousel. The connections of axis are shown in detail.

thermal expansion is employed. The clutch made of aluminum contracts more than the axes made of nonmagnetic steel. Thanks to different thermal expansion the rigid and tight connection is ensured.

The axis of 5 mm in diameter is thereafter separated again because of connection of two flanges. This axis is limited by its offset in motion downstairs and turns in

drilled hole in the flange. At the end of both axes there is a half bevel in normal direction whereby the connection of axes is performed. The connection is depicted in detail in Figure 6.3. The propelled axis continues next in the carousel sample holder, where it carries and propel a pinion. This axis is ensured in the right position by offset on both sides.

### 6.1.3 Gears

To propel the carousel the spur gears distinguished by simple design and fabrication are employed. For propulsion of the carousel, the small clearance is necessary. Nevertheless, thanks to the optimal choice of a module the clearance between the pinion and the wheel can be gained very small. Another requirement deals with the fast and easy changing of the samples which are placed inside the carousel. Due to this fact, the tothing is directly manufactured in the carousel which is directly inserted in teething pinion.

The mechanism of carousel sample holder does not transfer big torque, therefore the strength calculation of toothed gears is useless. For the design of housing of carousel sample holder, only the basic calculations of gears were performed. The smaller wheel is called the pinion and it is designated by an index one. The bigger one is called the wheel and it is designated by an index two. All necessary parameters of the gears are depicted in Figure 6.4.

The proposal of gears lies in several steps of calculations. Firstly, the choice of a module is necessary to define. The module is a basic characteristic of the tooth and its values are normalized by the standard ČSN 01 4608 [50]. The module was chosen  $m = 0,5$  mm. The distance between the middle of the carousel and the side of housing allowed the maximum suitable diameter of a gear  $d_{a2} = 24$  mm. In case of the pinion, the effort was to place it as close as possible to the side of the housing from the reason of increasing distance between the microwave waveguide and the propelled axis. This fact is useful for the proposal of propulsion of carousel because of the size of the clutch and of the perpendicular gears. The maximum possible diameter of the pinion is  $d_{a1} = 9,5$  mm.

The calculation are based on the following equations [50]

$$p = m \cdot \pi, \quad (6.1)$$

$$s = \frac{p}{2} = e \quad (6.2)$$

$$i = \frac{d_2}{d_1}, \quad (6.3)$$

$$z = \frac{d}{m}, \quad (6.4)$$



$$a = \frac{d_1 + d_2}{2}, \quad (6.5)$$

$$h_a = m, \quad (6.6)$$

$$h = 2,25 \cdot m, \quad (6.7)$$

$$d_a = d + 2 \cdot m, \quad (6.8)$$

$$d_f = d - 2,5 \cdot m, \quad (6.9)$$

where the pitch  $p$  expresses the distance of two identical points between two neighbouring teeth and  $s$  is the tooth thickness. The gears ratio is  $i$ , the number of teeth is noted as  $y$  and the distance between axes of the pinion and of the wheel is  $a$ . The addendum  $h_a$  indicates the height of tooth head and the dedendum  $h$  height of tooth root. The tip diameter  $d_a$  expresses the maximum diameter of the pinion or the gear and the root diameter  $d_f$  designates the minimum diameter. The face width of the pinion is  $b_1 = 2$  mm and in case of the gear it is only on the bottom side. The reference diameter is expressed by  $d$ . All calculated parameters are mentioned in the followed table 6.1.

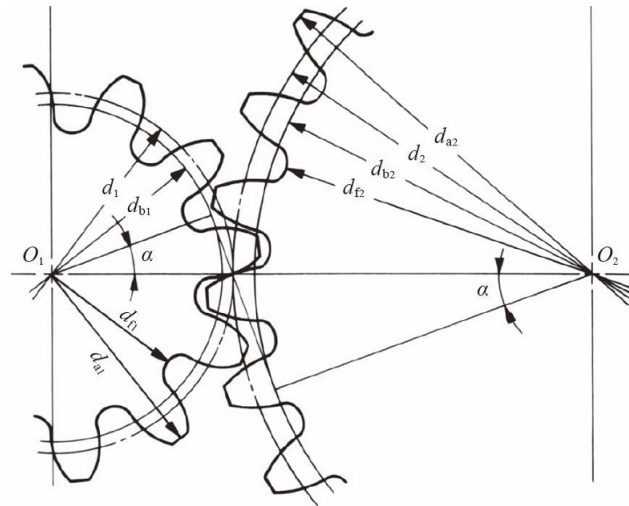


Figure 6.4: The scheme of gears with depicted parameters, The small wheel is called a pinion and the bigger one is called a wheel. Taken from [50].

### 6.1.4 Optical Sensor of Position

To determine the precise position of the sample in the carousel, the newly designed encoder is used. The encoder is based on principle of optics. The optical sensor is developed in cooperation with NETWORK GROUP s.r.o. [51] company, which is also responsible for supplying each component.

Table 6.1: Calculations of gears parameters. All parameters are in millimeter unit.

$d_1$	$z_1$	$d_{a1}$	$d_{f1}$	$d_2$	$z_2$	$d_{a2}$	$d_{f2}$
8,5	17	9,5	7,25	23	46	24	21,75
$p$	$s$	$i$	$a$	$h_f$	$h$		
1,57	0,758	2,7	15,75	0,625	1,125		

Another type of detection, such as capacitive displacement sensor, could be also used. Nevertheless, the choice is limited by the nonmagnetic materials or principle of sensors. The position of the sample could be directly detected by the power unit. However, there were concerns about the accuracy of the position, plus it is not easy to recognize which type of sample is placed in the position for measurement. The problem with the determination of sample is caused by multiple separations of the propelled axis. There are too many connections, where the undesirable clearance can occur. For this reason, the encoder scanning directly the position of the carousel, was designed.

The simple principle of this system is depicted in Figure 6.5 a). The light beam is emitted by the source and it continuous through the optical fiber to the carousel. The beam comes from the fiber through surroundings to the small mirror, which reflects the light back into the optical waveguide. The reflected beam is subsequently led to the encoder, where the photodiode is placed. The photodiode records an illuminance. The evaluation of the carousel position is performed by comparison of illuminance between two light beams. One is reflected from the mirror and the other is reflected from the surface of the carousel. Moreover, small mirrors with different reflectance from the surface can be placed into the carousel. These mirrors can not have the same reflectance as the surface of carousel. Due to this fact, the information what kind of sample is currently turned in the right position can be gained. The expected profile of the curve of the illuminance to the angle of turn of the carousel is plotted in the diagram in Figure 6.5 b). The mirror has a small hole inside, which creates a small gap in the diagram. Thanks to the small hole, the accuracy is ensured. The carousel is depicted in Figure 6.5 c).

For adequate accuracy of the position, the optical fiber has to be led to the surface of the carousel or of the mirror as close as possible. The ideal distance should be constant during the whole detection and its size is 1 mm. From this reason, the mirrors are put in a small drilled holes in the carousel. Due to the small distance between sonde and carousel, the sonde has to be made removable and it has to be pulled out from the sample holder during every sample exchange.

The problems of this system occur because of applying of the optical fiber, fixed and led in thin pipe from the connector to the carousel, at low temperature. At

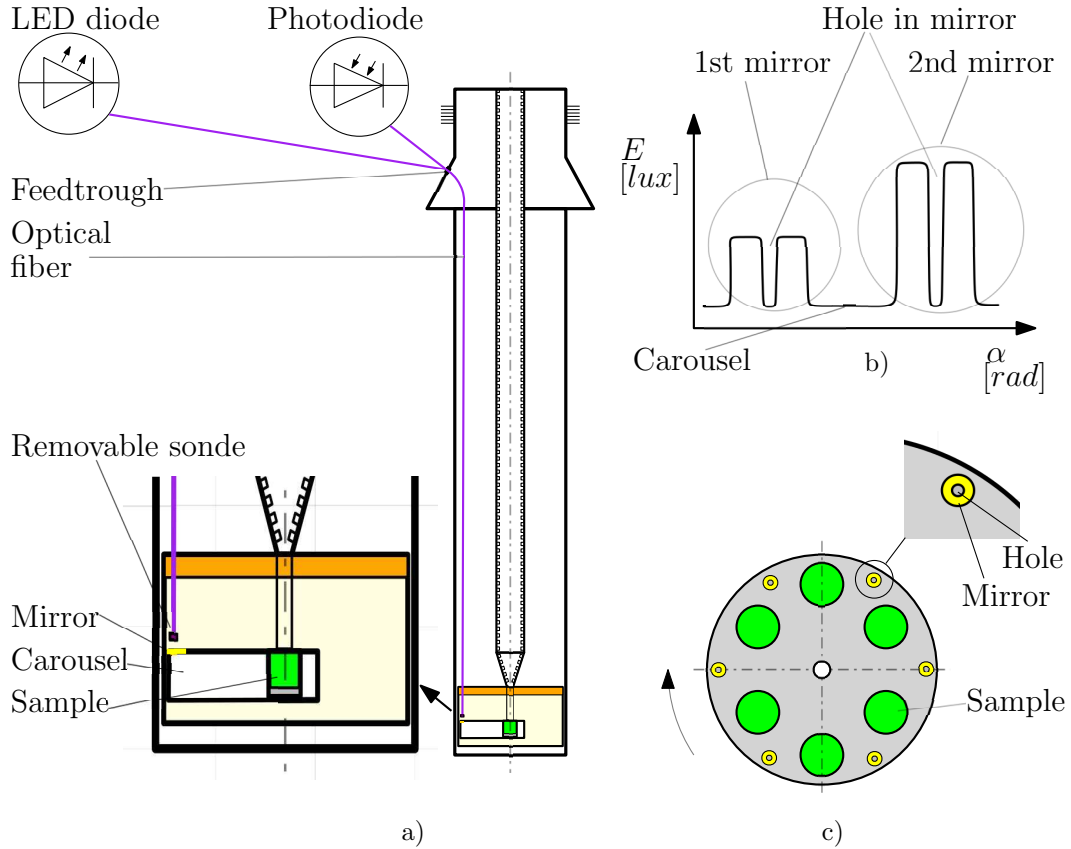


Figure 6.5: a) The schematic description of optical sensor of position, b) the profile of curve of illuminance to the angle of turn of carousel, c) scheme of carousel with descriptions.

first, the optical waveguide has to be divided into two parts and then connected again. One part is placed in the room temperature and pressure and the second one is placed inside the superconducting magnet with its environment. It is necessary to ensure that the cryostat is hermetically closed. Therefore, the optical feedthrough for vacuum and low temperature has to be applied.

It could seem that another complication may occur because of the placement of the optical fiber at the low temperature [52]. Nevertheless, the optical fiber and its bending properties are not affected by low temperature [53].

### 6.1.5 Modulation Coil

For amplification of the signal, the modulation coil, which consists of many turns of copper wires, is applied [22]. The principle of the coil is based on creating of the magnetic field around the wire, where the current flows. The demanded modulation magnetic field  $B$  should be up to 40 G with the frequency up to 100 kHz. The

supply current, as small as possible, is suitable because with the increasing current, the larger amount of heat that the coil produces, is released. The optimal supply current is commonly 0,7 A or less.

The conventional types of coils, which are sufficient to produce the required magnetic field, are frequently used. Consequently, the simple coil was employed for the earliest proposal. But the carousel in HF-EPR spectrometer is placed on one side in the sample holder and for utilizing of the maximum number of samples, it is necessary to use carousel with maximum diameter. Therefore, the dearth of space compelled to choose another suggestion of coil.

The solution of right choice of modulation coil lies in use of Helmholtz coil <sup>1</sup>. It is consisted of two simple circular magnetic coils, which are symmetrically aligned with mutual axis. The distance  $h$ , taken from the centre of coil, is the gap between these coils and it is equal to the radius of the coil ( $h = R$ ). When the distance and the radius are different, the inhomogeneity of magnetic field occurs [55], [56]. Both coils are made with the same radius  $R$  and the same electric current in the same direction. The maximum of magnetic field is situated in the center of both coils, as it is shown in Figure 6.6 a).

The fundamental principle of Helmholtz coil is described by several equations [54]. The magnetic field  $B$  is expressed by equation:

$$B_z = \frac{\mu_0 N I r^2}{2} \left( \frac{1}{(z^2 + r^2)^{3/2}} + \frac{1}{((d - z)^2 + r^2)^{3/2}} \right) \quad (6.10)$$

and for the configuration when  $d = r$  it is simplified by:

$$B \approx \frac{8,99 \cdot 10^{-9} N I}{r} \quad (6.11)$$

where  $N$  indicates the number of turns (same for each coil), the  $I$  is current and  $r$  expresses the coil radius.

The important parameter for the Helmholtz coil of frequencies up to 100 kHz is the cell inductance, equation 6.12 [54]. It expresses the sum of mutual inductance between two coils  $M$ , equation 6.13 and series inductance for each coil  $L$ , equation 6.14. The equations are shown below:

$$L_{Total} = 2(L + M), \quad (6.12)$$

$$M = \alpha N^2 r, \quad (6.13)$$

$$L = N^2 r \mu_0 \left( \ln \left( \frac{16r}{a} \right) - 2 \right), \quad (6.14)$$

---

<sup>1</sup>Helmholtz coil is named after the German physicist H. von Helmholtz [56].

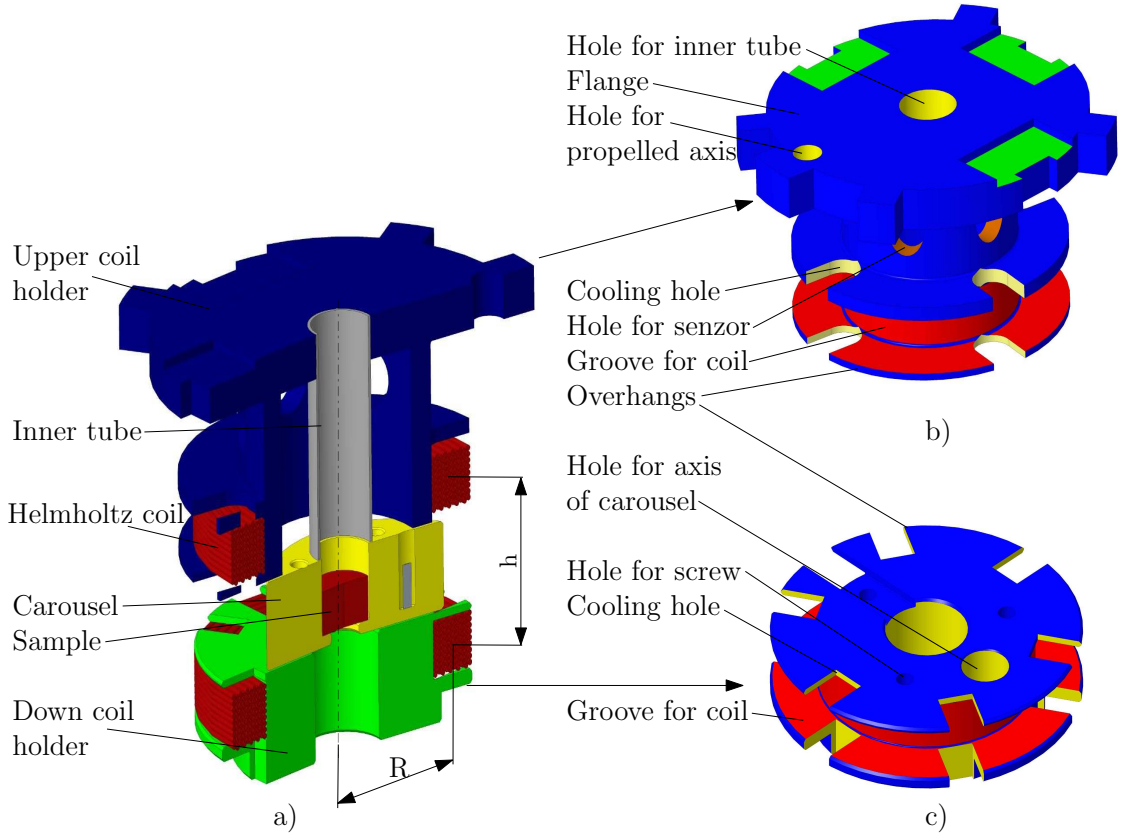


Figure 6.6: The designed Helmholtz coil with description of each parts. a) the coils are placed on the basis of the rule  $h=R=11,2$  mm, b) the upper coil holder including the flange of carousel sample holder, c) the down coil holder as a support for axis of carousel.

where the permeability of free space is expressed by  $\mu_0$ ,  $\alpha$  is a constant and  $a$  indicates the diameter of wire bundle cross section [54]. The total inductance is directly proportional to the number of turns, therefore, the number of turns must be as small as possible. The ideal value of inductance is up to one, but the permissible value is two. In case of proposal the inductance is equal to 1,8 mH [54].

The frequency  $f$  can be calculated by using equation 6.15, where the coil interwinding capacitance is designated by  $C_O$  and the coil capacitance to ground is  $C_G$  [54].

$$f = \frac{1}{2\pi\sqrt{(L + M)(C_O + C_G)}} \quad (6.15)$$

The central point of the magnetic field is situated in the center of the sample. Moreover, the magnetic field evinces the distribution of magnetic field also near the central point. In Figure 6.7 the range of distribution is depicted.

The interesting thing lies in the similar shape of the curves, therefore, the ho-

mogeneity of magnetic field has basically the same values in the horizontal and vertical direction. The magnetic field with similar value is in the range plus or minus one millimeter. At the higher distance between the sample and coils, the magnetic field decreases. In HF-EPR mirrors, half or one millimeter thick, are used. Nevertheless, from diagram 6.7 follows that the center of magnetic field can be moved about one millimeter. Therefore, the possibility of using the different thickness of mirrors.

Helmholtz coil is placed as close as possible to the sample because it is necessary to apply the coils with the diameter as small as possible. All these parameters come from the precondition, that the emitted heat from the coils must be negligible due to cooling of the magnet. From the equations follow that with more turns, the bigger supply current is needed. With using the bigger supply current, the bigger heat is created. From these reasons, both types of coil holders have milled holes, where the cooled stream can flow. The coils holders are made of copper because it has favourable thermal conductivity. So the coil holders can transfer heat to the surrounding.

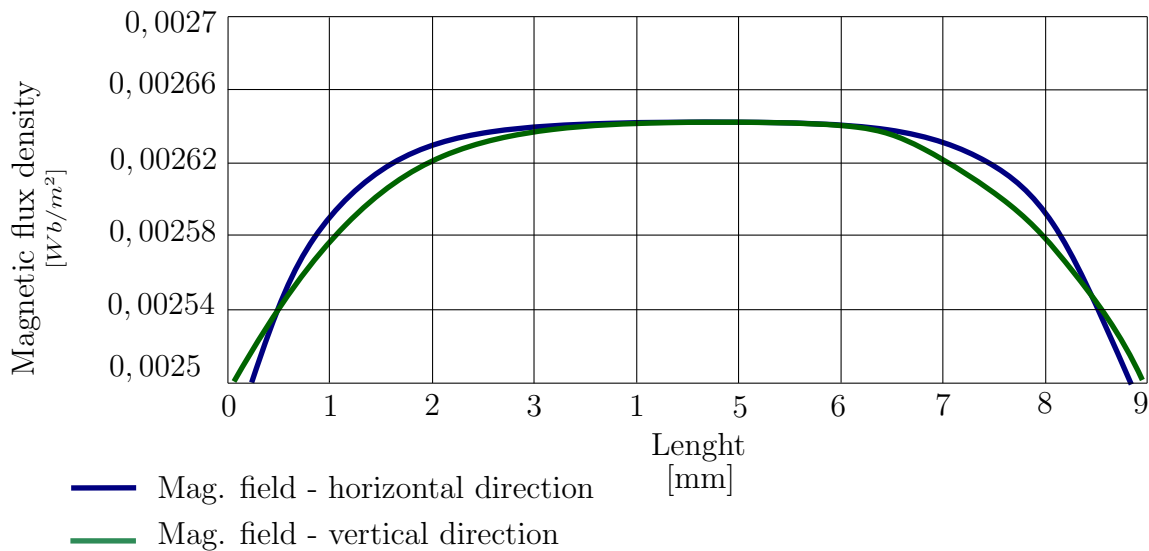


Figure 6.7: The diagram of the magnetic field and the length in vertical and horizontal direction. The blue line designates the horizontal direction and the green one indicates the vertical direction. The homogeneity of magnetic field is in the range 2 mm.

For Helmholtz coil, two specific coil holders are designed. There is only one possibility for their implementation. The lower coil holder consists of one part inserted into the housing of sample holder and connected by three screws. Lower coil holder, which is depicted in Figure 6.6 b), contains the groove all around, where the wires are placed. The holes for cooling are drilled from the bottom side. The

upper section of coil holder has the longitudinal holes because of heat cooling and for current supply. The upper coil holder, which is depicted in Figure 6.6 c), has another shape because it carries the connectors for wires and it is the component containing the flange of the sample holder. The coil itself is placed in the hollowed groove all around. The position of the upper coil holder is ensured by overhangs, which are tightly inserted into the holes in the housing of sample holder. The upper coil holder is fixed in the vertical direction by opposite flange, by the taper one. Moreover, through the flange, the propelled axis is leads. For the reason of sensors, the holes are drilled from the side inwards.

Each Helmholtz coil is made of 72 turns of a 0,3 mm diameter copper wire (0,4 mm diameter with isolation). The radius  $R$  of the middle of coils is 11,2 mm and the distance between them  $h$  has the same value. The groove for the coil has a squared shape with the size of edge 3,5 mm. A maximum modulation field of about 4 G (for a 700 mA current and 10 V voltage) can be reached with the power supply by a amplifier NI PXIe-4610 from a company National Instruments (Figure 6.8) [57].



Figure 6.8: The power supply fo Helmholtz coil from the National Instruments company. Taken from [57].

### 6.1.6 Description of Assembling

The carousel sample holder is directly connected to the flange of corrugated taper by the locking system. The flange of corrugated taper fits closely into the top of housing and to the upper coil holder. All these components are aligned by circular overhangs and only one possibility of their assembling is ensured by one pin. The unsymmetrical shape of coil holder allows only one possible implementation.

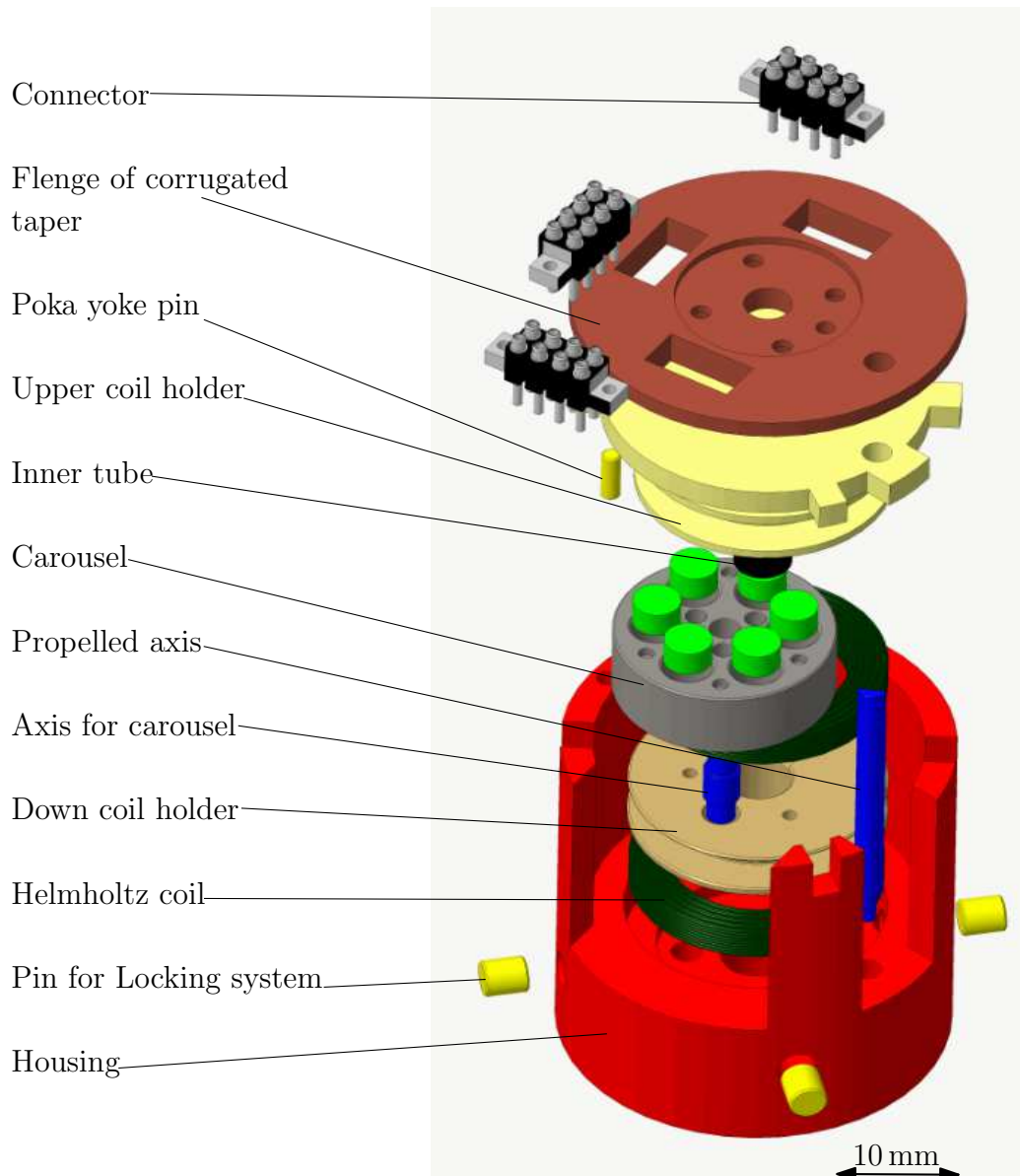


Figure 6.9: The assembly of the carousel sample holder.

The basic part of carousel sample holder is named housing (Figure 6.10) and it carries all components needed for the functionality of sample holder. The shape of the housing is adjusted to demands of all used parts placed inside. The rectangular gaps on the sides of the housing are employed due to less massiveness of this part. It causes the shorter time of cooling. Also, this free space helps for inserting of carousel during its exchange. The down section of the housing includes several holes, which are used for down coil holder especially for its ensuring by screws. The remaining holes help with better recirculation of Helium inside the holder.

Thanks to the carousel (Figure 6.11), the measurement of more samples can be



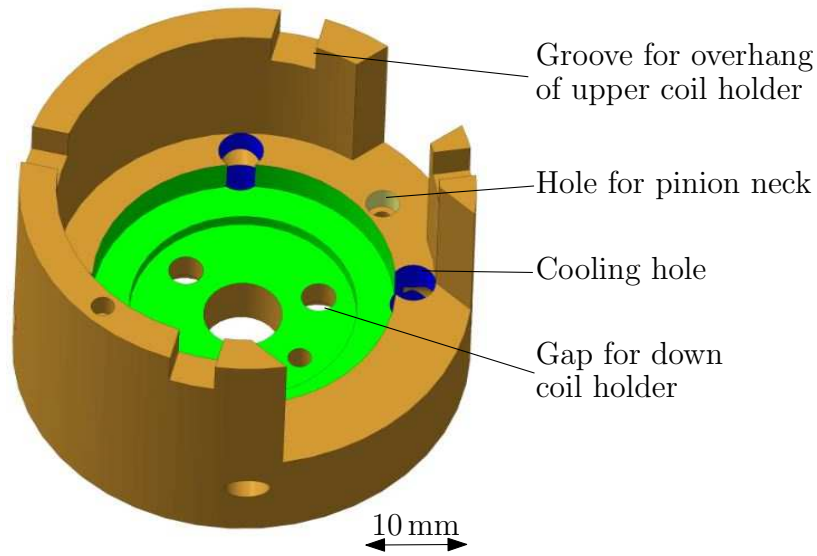


Figure 6.10: The housing of carousel sample holder. The varied shape is caused because of the implementation of other components.

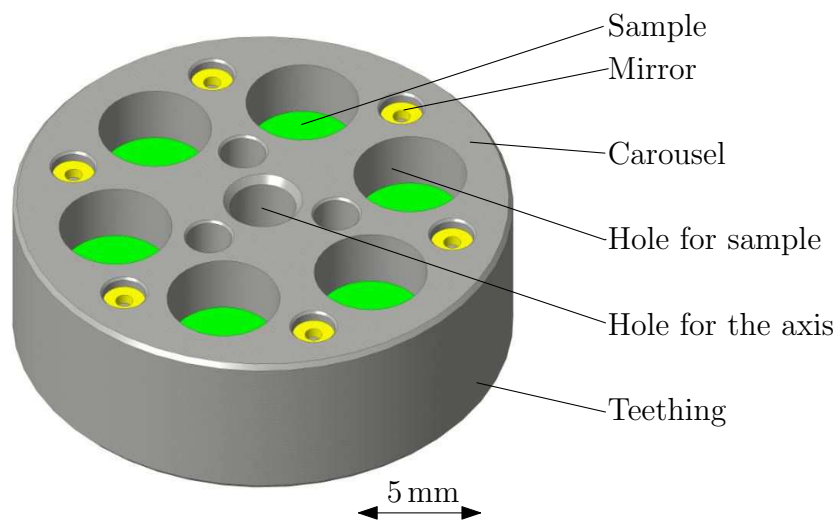


Figure 6.11: The description of carousel for six samples put on the axis. The carousel is propelled by gears and its position is measured by the reflected sensor.

realized. As an optimal number of samples was chosen six because of suitable ratio of utilizable space to maximum number of samples. Generally, the carousel has a circular shape with many drilled holes and it is put on the axis. The axis goes through the down coil holder up to the housing. Its next task is also to ensure the correct positioning of mentioned components. For propulsion of carousel, the tothing around is employed (see subsection Gears 6.1.3). The movement of the

carousel in vertical axis downward is limited by the widening of the axis, therefore, the carousel does not touch the down coil holder. However, in the direction upward the movement is not limited because of the sample exchange. From this reason, the carousel sample holder cannot be turned a head down.

The samples are placed into the drilled holes of the carousel and their appropriate position is delimited by offset inside the holes. The thickness of this offset is as thin as possible due to utilizing of Helmholtz coil (see subsection Modulation Coil 6.1.5). The smaller holes inside the bottom of the sample are drilled because of the better cooling of the sample and for the easier sample exchanging. The hole for the sample is eight millimeters deep, therefore, various types of mirrors or of samples can be used. On the top of the carousel, the holes for mirrors are drilled. The holes are subsequently utilized for detection of the position of the sample (see subsection Optical Sensor of Position 6.1.4).

### **6.1.7 Sample Exchange**

For exchange of the sample is necessary to take the carousel out from the carousel sample holder. Due to this fact, the locking system has to be disconnected and the whole sample holder has to be taken out. From the carousel sample holder, it is necessary to take out the upper coil holder. Because of using wires and sensors which are directly connected to the coil holder this step has to be performed with a caution. The carousel lies tightly above the lower coil holder and it is put on the carousel axis, from which the carousel is necessary to take out.

For itself exchange of the samples, a simple change stand may be used. It is composed of a plastic base and of six regularly placed pins, depicted in Figure 6.12. The carousel can be placed into the change stand on several pins. For better ensuring of carousel placing the chamfer on the inner diameter of the stand is employed. Thanks to this the carousel slides into the exchange position. When the carousel is pressed down, the pins push the samples up. Therefore, the samples are relaxed and ready for replacing with other ones. Before inserting of new sample inside the holes of carousel, the carousel has to be lifted up from the change stand and it should be subsequently put out, for example on the table. The sample is ensured inside the holes due to small clearance between the sample and drilled hole. Therefore, the sample has to be forced into the right position in the hole. Beneath the sample, the mirror is used, but it is very often including part of the sample.

The insertion of carousel into the carousel sample holder is performed in reverse direction as it is mentioned above. One step, in addition, is maybe good to perform, it is good to take a photo of the carousel before its inserting into the housing of carousel sample holder.

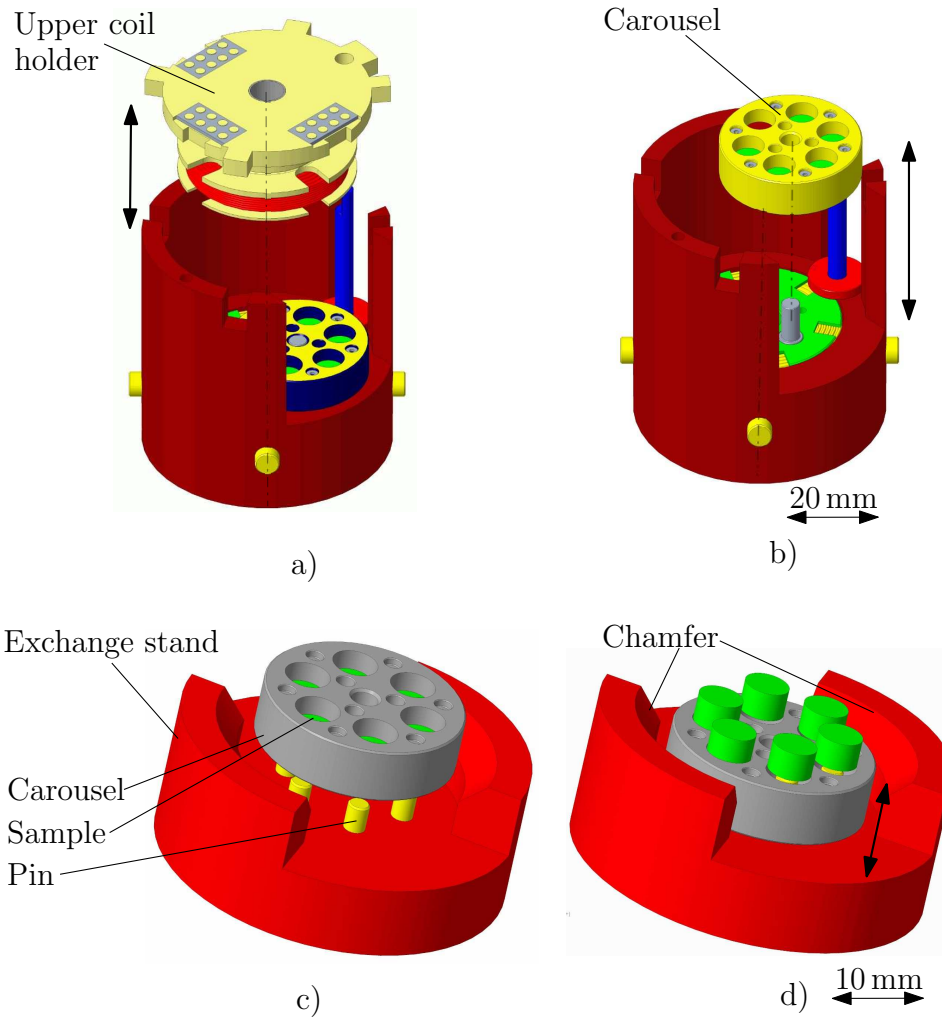


Figure 6.12: The particular figures show the individual steps needed for the exchange of the sample. a) for changing has to be removed upper coil holder, b) the carousel including samples is necessary to take out from the holder, c) for pushing of the samples from the carousel, the exchange stand can be applied.

### 6.1.8 Simulation of Gaussian Propagation for Carousel Sample Holder

One of the very important points is that all components of the sample holders have to be very precisely aligned (see the section Beam Coupling 3.4). Otherwise, the losses of microwave power occur. The correct coupling of parts can be known thanks to the simulations. The simulations of microwave propagation were run using a software ANSYS HFSS 14.0 [58] which is compatible with the software CST Studio [59]. Due to high difficulty of the microwave calculations for computational capacity the simulations were created in cooperation with specialists from the company Thomas

Keating Ltd [48].

The problem with adequate beam coupling occurs because the inner tube cannot achieve totally to the upper side of the carousel. This is caused by rotating motion of carousel. The large size of the gap can cause high microwave power losses. Therefore, the distance between the end of the inner tube and the upper surface of carousel has to be as small as possible. From the previous experience of sample holders, the desired distance is 0,3 mm. Therefore, there was no effort to use another size. The Figure 6.13 shows the divided waveguide from inside face of the hole for the sample in the carousel.

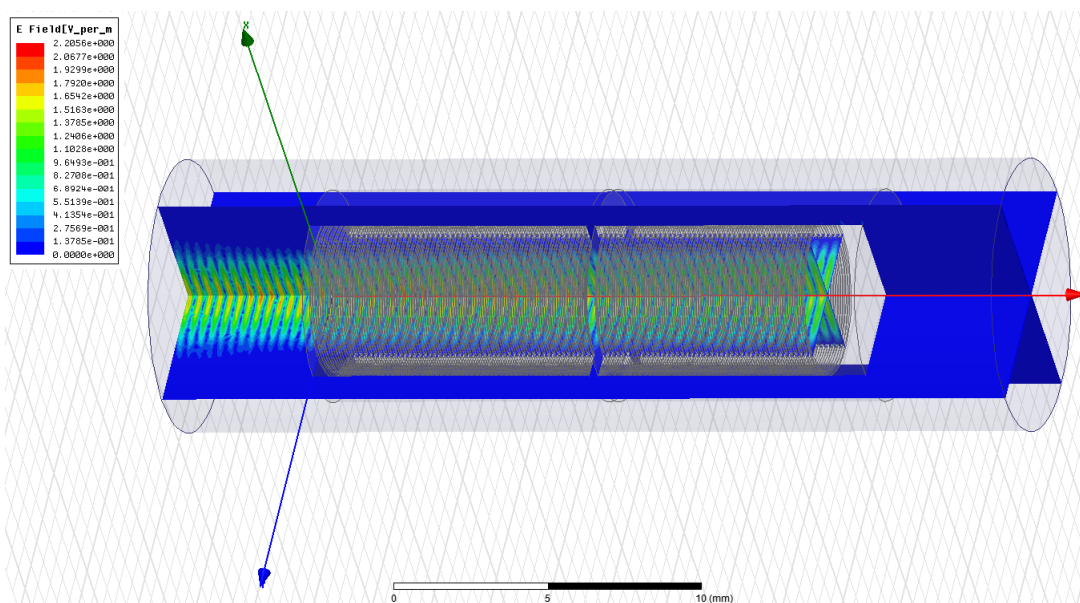


Figure 6.13: The simulation of microwave radiation through the waveguide. The gap is caused by connection of waveguide to carousel.

From Figure 6.13 is evident that at the gap is no visible electric field leakage. This is because the beam is parallel across it (the wavelength is small compared to the width of the waveguide). The maximum intensity of electric, respective magnetic, component is situated in the middle of the waveguide. For both components are considered, where the electric field is maximal, the magnetic field is minimal, and vice versa. On the walls of the waveguide, the intensity of microwave radiation is negligible.

The simulation dedicates that the gap 0,3 mm high between the end of the inner tube and the upper face of the carousel can be applied.

## 6.2 Rotating Sample Holder

The design of the rotating sample holder lies in an improvement of the currently used type of sample holder. The range of rotation used for measurement of the sample is  $360^\circ$ . The bigger size (50 mm) of superconducting magnet allows using bigger but simpler sample holder. Therefore, the new design of the rotating sample holder was suggested.

The current used rotating sample holders mostly use propulsion unit placed at the bottom of the holder. Because of placement of propulsion unit, it is necessary to use gears or another sophisticated mechanism for propulsion of rotary shaft. However, gears cause creating of clearances. The bigger size of magnet allows using directly the piezoelectric rotator without utilizing gears. The shaft is directly propelled by the rotator. Therefore, the even smallest clearances do not occur.

The next advantage consists in the shorter time needed for cooling of the rotating sample holder. Due to direct propulsion, fewer components, which have to be cooled, are used. Therefore, the whole time of measurement is reduced. Due to this fact, also the costs of rotating sample holder and of demanded energy are lower.

The whole assembly is depicted in Figure 6.14, where all components are described.

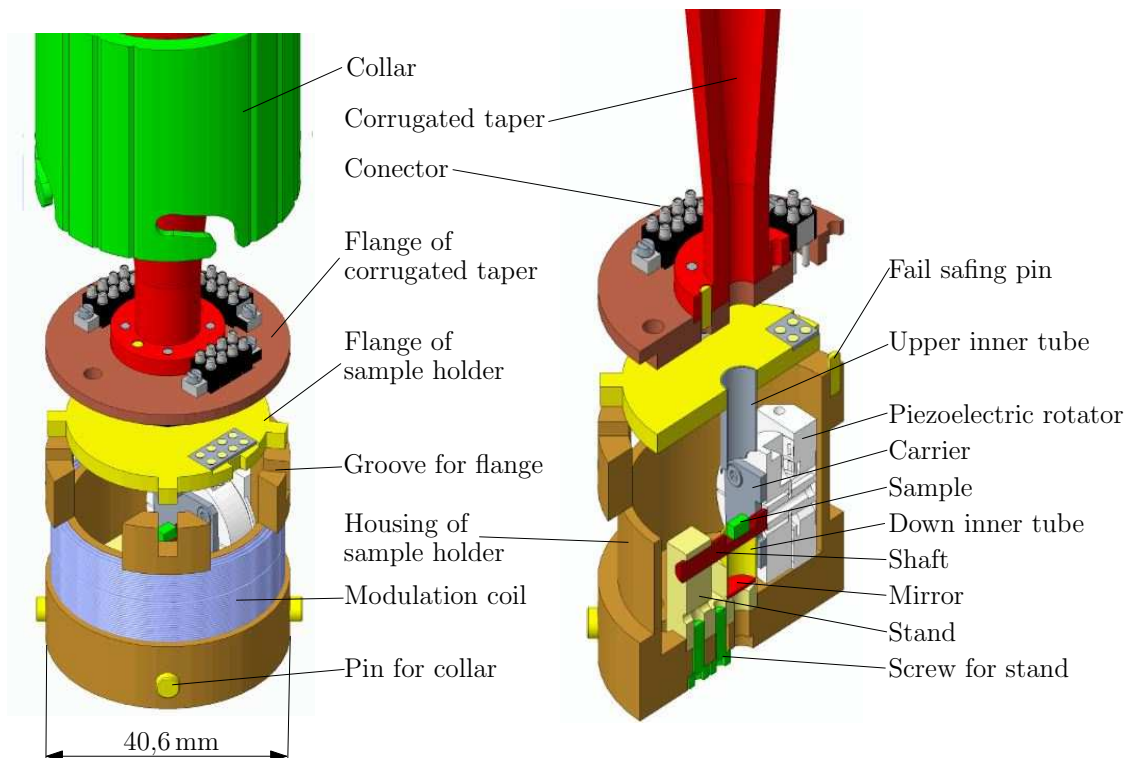


Figure 6.14: The rotating sample holder with described individual components.

### 6.2.1 Description of Assembly

The rotating sample holder, depicted in Figure 6.14, is directly connected to the flange of corrugated taper by locking system described previously in the carousel section 5.3. To avoid misalignments, the flange of rotating sample holder is embedded two and half millimeters inwards the housing of sample holder. Therefore, the flange of the corrugated taper fit closely into the housing. The pin on the top of the housing is designed for the assembling of these two parts. Thanks to this, the rotating sample holder can be joined in only one direction.

The housing which carries and covers all necessary components, is the main part of the sample holder. The housing has the circular shape needed for utilize inside the magnet. For better heat exchange between the environment inside the rotating sample holder and the environment in the magnet, the housing has drilled gaps on the sides. These gaps are covered by collar, nevertheless, the less material means the less energy for cooling. Moreover, at the bottom of the housing four holes are drilled, which helps for better flowing of Helium inside the rotating sample holder (Figure 6.15). At the bottom, the stand the shaft is also placed.

For measurement of the sample, the high stability and precision of the position of the shaft are necessary. Therefore, the position of the stand is very important. It is inserted into the hollowed gap for stand. This gap has drilled holes in each corner to avoid of creating the radius in the corners. Even small radius in the corner can cause a shift of the stand and subsequently of the shaft. These four holes also help for better cooling inside the sample holder. The housing has the supports for the flange and for connection with the flange of corrugated taper. The supports have small unsymmetrical grooves on the top, where the flange is inserted.

The flange of rotating sample holder carries the connectors and the upper inner tube. It constitutes a bridge above the system of propulsion and the sample. The upper inner tube is solidly fixed in the hole in the middle of the flange. This flange has unsymmetrical shape of overhangs depicted in Figure 6.15, which can be inserted into the grooves on the top of housing.

The individual components are described in next sections.

### 6.2.2 Propulsion System

The rotary movement is ensured by the piezoelectric rotator Attocube ANRv51 [60] depicted in Figure 6.17, which allows very precise adjustment of rotary movement with resolution in milliradians. The rotator is made of nonmagnetic materials and it is able to endlessly turn the shaft with the horizontal rotation axis. Moreover, this rotator is appropriate to be used at low temperatures. For its control is necessary to use five wires. Two wires drive the piezo and three wires read the position. The

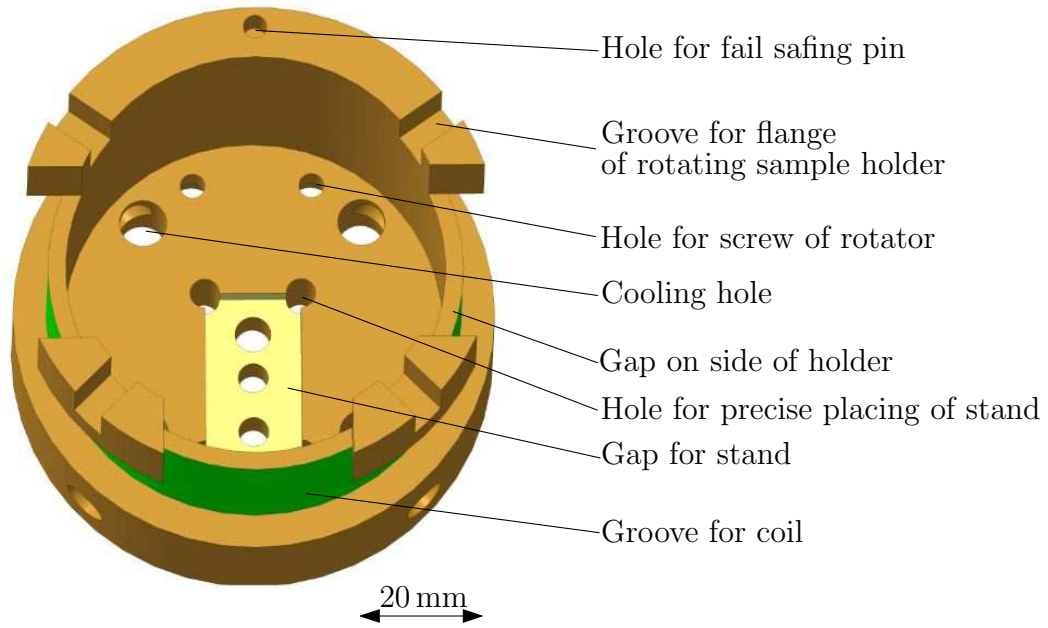


Figure 6.15: The housing of the rotating sample holder is the main part of holder. The shape of it is adapted to other components placed inside.

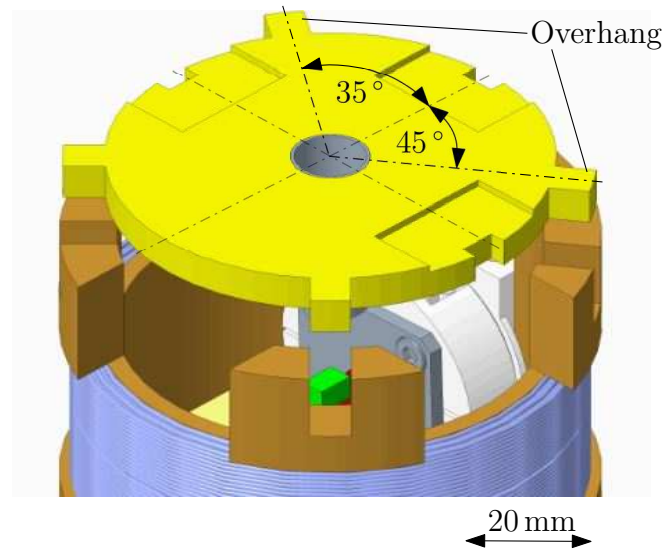


Figure 6.16: The schema of flange with unsymmetrical shape of overhangs.

range of rotation is  $360^\circ$ . However, not full range of rotating detection is covered. The encoder of piezoelectric rotator is able to read out only in range  $0^\circ$  to  $340^\circ$  [60].

The piezoelectric rotator is solidly connected to the housing by two screws depicted in Figure 6.14. It propels the shaft, where the sample is placed. Because of concerns about a damage of the rotator, the shaft is supported by one solid itself

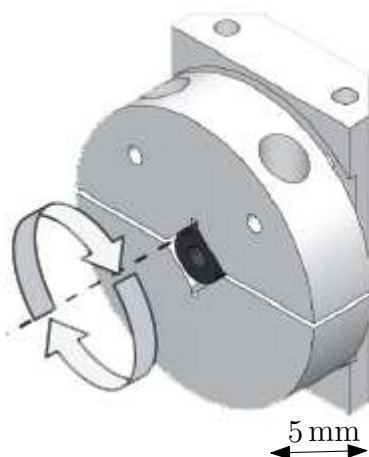


Figure 6.17: The rotary piezoelectric rotator ANRv51 from company Attocube. Taken from [60].

stand.

The transfer of torque is performed by the carrier, which propels the shaft by the tight longitudinal groove. The longitudinal shape is good for the optimal alignment of axes of rotator and the hole for the shaft in the stand. Thanks to the rectangular shape of one end of the shaft, the torque can be transferred. The position of the shaft in the axial direction is ensured by epoxy adhesive for cryogenic applications [61]. The shaft has material with the hollowed gap in the middle where the sample is placed.

### 6.2.3 Modulation Coil

As with the carousel sample holder, for amplification of the signal, the small oscillating field around the main magnetic field is used. The oscillating field is created by the modulation coil. The demanded parameters of the magnetic field are same as in case of carousel sample holder.

The use of Helmholtz coil seemed as an optimal choice for this purpose because their free space between coils offers more possibilities. The original effort dealt with the use of the same Helmholtz coil as was designed for the carousel sample holder. However, because of a dearth of space, the simple Helmholtz coil cannot be used.

Nowadays, the conventional types of rotating sample holders use the simple coil for creating the small magnetic field. For designed sample holder the simple coil in form of a solenoid is also used. The copper wire of the coil with the diameter 0.04 mm is directly wound in the groove around the outer diameter of the housing (Fig. 6.14). The position of the middle of groove corresponds to the position of



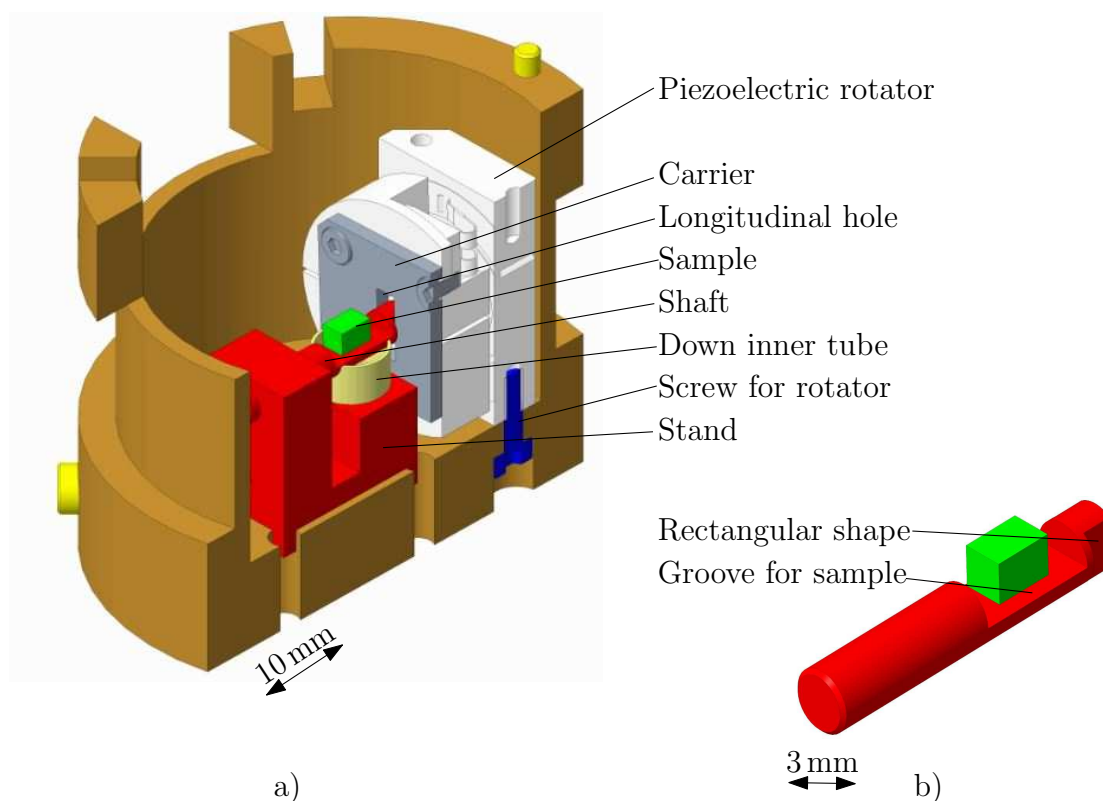


Figure 6.18: The propulsion of rotating sample holder. a) the rotating of the shaft is ensured by the piezoelectronic rotator. The coil holders are also the support of the shaft. b) the design of quartz shaft with half groove for the placement of the sample. The end, which is inserted into the longitudinal hole, has rectangular shape.

the sample due to creating of the homogeneous magnetic field. The coil is covered by the collar, therefore, the outer diameter of the coil cannot overhang the inner diameter of collar.

The coil with higher diameter produces the higher amount of undesirable heat inside. Nevertheless, the coil is placed on the outside of sample holder where the environment of cryostat can easily cool the coil.

### 6.2.4 The Sample Exchange

For observation of other samples, the exchange of samples is necessary to perform. Firstly, the locking system has to be unlocked and the rotating sample holder is subsequently taken out. The flange of rotating sample holder has to be also taken out. Afterwards, the sufficient free space for the exchanging is created.

The sample is fixed in hollowed gap by glue because the shaft can endlessly rotate around its own axis. The gaps on the sides of housing help for better handling with

the sample. For better and precise placement of new sample, a tweezer can be used. Then the rotating sample holder is connected again to the corrugated taper by locking system. The sample holder is ready for measurement. The main steps of the sample exchange is depicted in Figure 6.19.

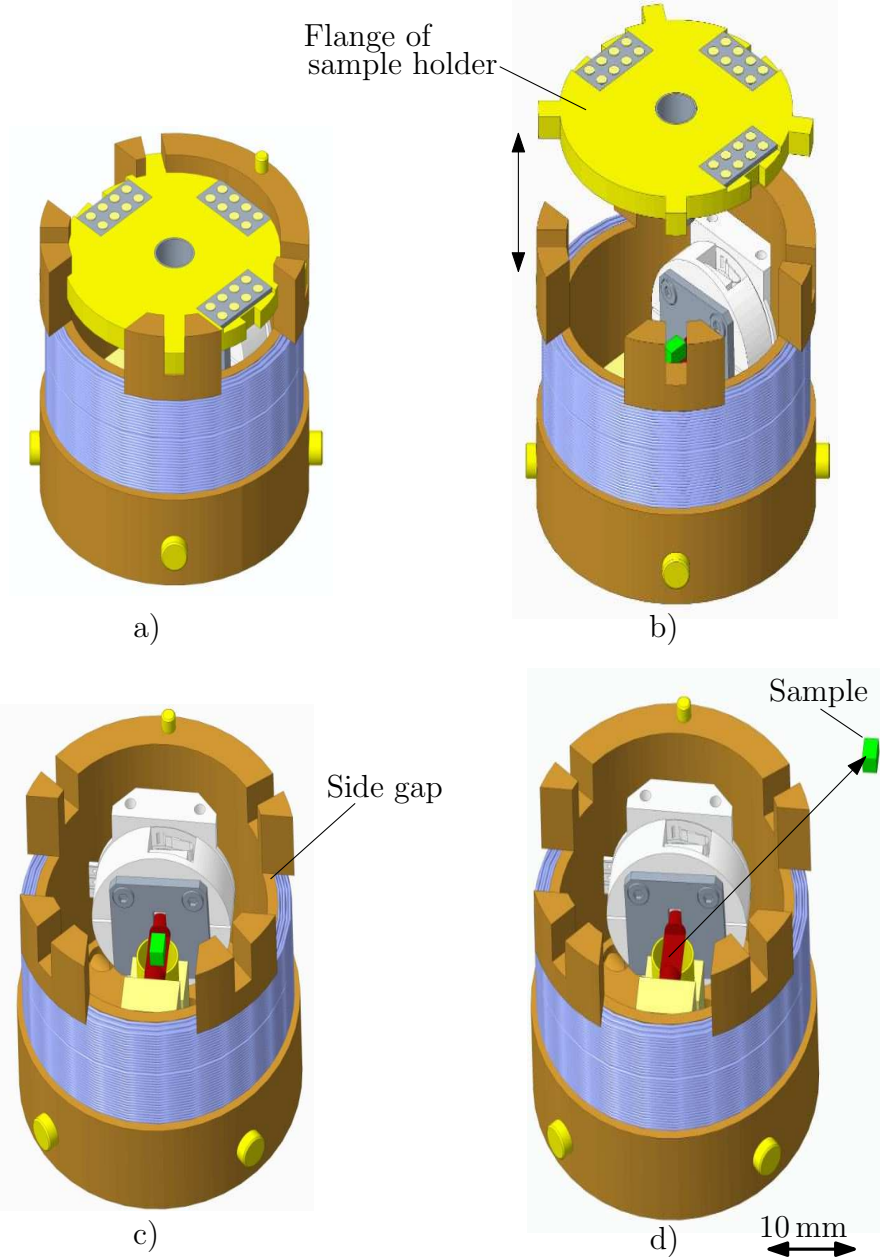


Figure 6.19: a) to exchange the sample it is necessary to unlock the locking system. b) the flange of rotating sample holder has to be taken out, c) afterwards the gaps on the sides of housing helps for easier handling with the sample. d) the sample can be taken out, for more comfortable handling the tweezer can be used.

## 6.2.5 Simulation of Gaussian Propagation for Rotating Sample Holder

The simulation of Gaussian beam propagation is also necessary to make for the rotating sample holder. Its base is similar to the simulation of carousel sample holder, nevertheless, the small hole ( $\phi 3$  mm) through the inner tube can constitute possible obstacle.

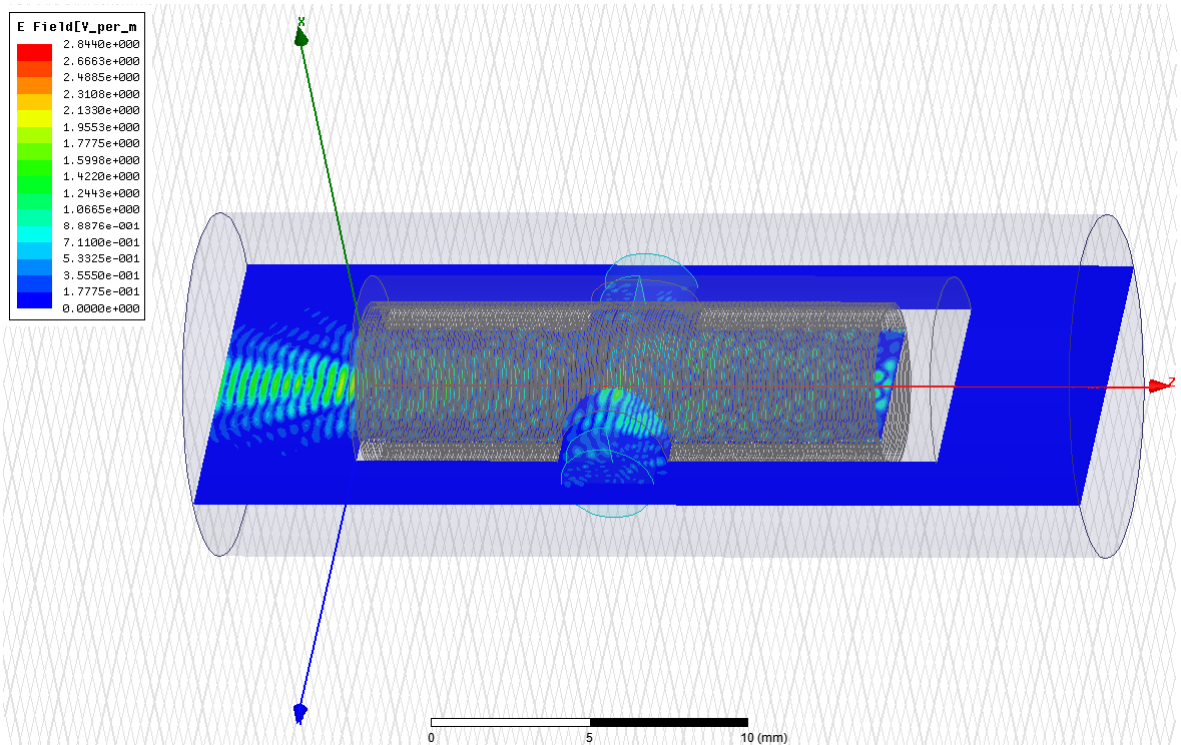


Figure 6.20: The simulation of microwave radiation. The hole on side of inner tubes is caused because of the shaft for sample. The sample holder is scattering the beam. The Gaussian beam is incident from the left.

The rotating sample holder includes the shaft which goes directly through the center of microwave propagation. To minimize the microwave power losses the shaft is made of quartz glass, which is very common utilized for this proposal [62]. The sample is not used for simulation and a gap of 0,3 mm to the waveguide (distance between upper and down inner tube). The result of simulation is shown in Figure 6.20 and the Gaussian beam is incident from left. In figure is depicted the reflected or refracted electric field. The field on the left of the figure ,therefore, represents the return signal to the detector. The reflected has a complex structure which indicates that the sample holder is scattering the beam.

To better imagine the situation with the shaft, the Figure 6.21 with description is depicted. The shaft is freely rotated in the hole consisted of semicircle of each inner tube. The shaft and the space from the side of inner tube (waveguide) causes creating deviation of the microwave propagation.

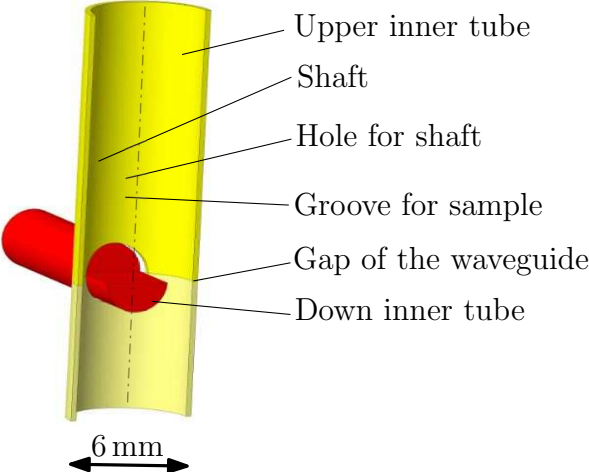


Figure 6.21: The cross section of the shaft goes through the upper and down inner tube. The shaft is directly placed into the microwave radiation.

## SUMMARY AND OUTLOOK

The presented master's thesis deals with the development of sample holders for EPR spectroscopy. The concept of this thesis is organized in the same way as the development was followed. Therefore, two separate parts are present, theoretical and practical part. Theoretical part is focused on EPR. The second part, practical part deals with sample holders design and can be divided into three parts:

Firstly, before the design of sample holders, in particular, the connection between the corrugated taper and the sample holder were suggested. Therefore, a new type of connection, the locking system with the turned collar, was designed. By this, tight and fast execution of connection was achieved. Moreover, the locking system can be implemented for various types of corrugated taper.

The chapter of carousel sample holder contained the whole overview of its development. The requirement of utilizing more samples during one measurement meant implementation of a sophisticated mechanism. It will be able to change samples and to place them in the center of microwave radiation during one measurement. From this reason, the rotary carousel propelled by axis, led from outside of magnet, was designed. Besides, the movable system demanded a sensor of the mechanism. Therefore, an optical sensor of a position of the sample was designed. For successful observation of the samples, the small magnetic oscillating field is necessary. Therefore, the choice and the placement of modulation coil played an important role in the design of modulation coil. The solution consisted in using of Helmholtz coil. The main obstacle during the designing of holder occurred due to lack of space because all components had to be squeezed into the pipe 44 mm in diameter.

Nevertheless, the designed carousel sample holder brought many benefits, such as considerable time savings (up to 50 percent of the time), the use of a reference sample (can be measured up to six sample per one shot), or the automation of the measurement process.

The next chapter dealt with the design of the rotating sample holder which brought also many advantages. The main lied in a very precise adjustment of the sample (in milliradians) thanks to the direct propulsion of piezoelectric rotator for the shaft. This is decisive for measurement anisotropic materials where the suitable tilt of basic crystal mesh is demanded.

The last sections of each chapter about the sample holders were dedicated to a functionality of holder. Therefore, both types of sample holders were checked by simulations. The results showed both holders are able to be used for measurement of the sample.



## BIBLIOGRAPHY

- [1] WEIL, J. A., J. R. BOLTON and J. E. WERTZ. *Electron paramagnetic resonance: elementary theory and practical applications*. 2nd ed. /. Hoboken, N.J.: Wiley-Interscience, 2007, 688 p. ISBN 978-0-471-75496-1.
- [2] Jeol: Solution for Innovation. *Joel* [online]. [cit. 2018-05-23]. Available from: <https://www.jeolusa.com/PRODUCTS/Electron-Spin-Resonance>
- [3] *Bruker* [online]. 2018 [cit. 2018-05-23]. Available from: <https://www.bruker.com/products/mr/epr/what-is-epr.html>
- [4] EMX USER'S MANUAL. Billerica, USA, 1998. Available from: <https://warwick.ac.uk/fac/sci/physics/research/condensedmatt/magneticresonancecluster/diamond-epr/facilities/epr/emx.pdf>
- [5] GERLACH, W. and O. STERN. *Zeitschrift für Physik*. 1922, 9 p. ISSN 353-355. Available from: <http://dx.doi.org/10.1007/BF01326984>
- [6] EATON, G. R., S. S. EATON and K. M. SALIKHOV. *Foundations of Modern Epr*. World Scientific. 1998. ISBN 978-9810232955.
- [7] PURCELL, E. M., H. C. TORREY and R. V. POUND. *Resonance Absorption by Nuclear Magnetic Moments in a Solid: Physical Review*. 1946, 69 p. Available from: <https://doi.org/10.1103/PhysRev.69.37>
- [8] HAINDL, E., K. MÖBIUS and H. OLOFF. *Z. Naturforsch.* 1985, 40 p.
- [9] HALLAK, F. E., J. van SLAGEREN and M. DRESSEL. *Torque detected broad band electron spin resonance: Review of Scientific Instruments*. 2010. DOI: 10.1063/1.3482158.
- [10] PRISNER, T. and W. KÄOCKENBERGER. *Application Magnetic Resonance*. 2008, 34 p.
- [11] Vzpomínky na NMR v Brněnské Tesle. *Stan's NMR Blog* [online]. 2008 [cit. 2018-05-23]. Available from: [http://www.ebyte.it/library/hist/NMR\\_Tesla\\_cs.html](http://www.ebyte.it/library/hist/NMR_Tesla_cs.html)
- [12] KERN, M. *Optical setup for torque detected electron spin resonance spectroscopy*. Brno, 2015. Master-s thesis. Brno University of Technology, Faculty of Mechanical Engineering. Vedoucí práce Dr. Ing. Petr Neugebauer.

- [13] FUCHS, M. R. *A High-Field / High-Frequency Electron Paramagnetic Resonance Spectrometer (360 GHz / 14 T)*. Berlin, 1999. Ph.D. thesis. Freie Universität Berlin.
- [14] NEUGEBAUER, P. *Development of a Heterodyne High Field / High Frequency Electron Paramagnetic Resonance Spectrometer at 285 GHz*. Grenoble, 2010. Ph.D thesis. University of Grenoble.
- [15] REIJERSE, E. J. *Journal of Magnetic Resonance*. 1995, 37 p.
- [16] GOLDSMITH, P. F. *Quasioptical systems: Gaussian beam quasioptical propagation and applications*. Piscataway, NJ: IEEE Press, 1998, 430 p. ISBN 978-0-7803-3439-7.
- [17] LYNCH, W. B., K. A. EARLE and J. H. FREED. *Advanced EPR, Applications in Biology and Biochemistry*. Amsterdam, 1989, 307 p.
- [18] PRISNER, T. F. *Advances in Magnetic and Optical Resonance*. 1997, 20 p.
- [19] SMITH, G. M., J. C. G. LESURF, R. H. MITCHELL et al. *Review of Scientific Instruments*. 1998, 69 p.
- [20] COLLIN, R. *Foundations for Microwave Engineering*. Second Edition. New York: John Wiley, 2000.
- [21] BUDIL, D. E. and K. A. EARLE. *Sample Resonators for Quasioptical EPR: A Practical Guide for Biological Applications*. 2004. ISBN 978-1-4419-3442-0.
- [22] BUDIL, D. E. and K. A. EARLE. *Sample Resonators for Quasioptical EPR: A Practical Guide for Biological Applications, vol 22*. 2004.
- [23] *Optiforms* [online]. Temecula [cit. 2018-05-07]. Available from: <https://www.optiforms.com/resources/what-is-electroforming/>
- [24] HASSAN, A. K., A. L. MANIERO et al. *High-Field EMR: Recent CW Developments at 25 Tesla, and Next-Millennium Challenges*. 1999.
- [25] KUTTER, C. *Pulsed Electron Paramagnetic Resonance in High Magnetic Fields using Far Infrared Lasers*. Konstanz, 1995. Ph.D. thesis. Freie Universität Konstanz.
- [26] POOLE, C. P. *Electron Spin Resonance: A Comprehensive Treatise on Experimental Techniques*. Second edition. New York: Dover, 1997.



- [27] STOLL, S. and A. SCHWEIGER. EasySpin, a comprehensive software package for spectral simulation and analysis in EPR. *Journal of Magnetic Resonance*. 2006. Available from: <https://doi.org/10.1016/j.jmr.2005.08.013>
- [28] GOLISH, D. R. *Quasioptical Systems and Components for Terahertz Astronomy*. Arizona, 2008. Ph.D thesis. The University of Arizona.
- [29] FUCHS, M. R., T. F. PRISNER et al. *A high-field/high-frequency heterodyne induction-mode electron paramagnetic resonance spectrometer operating at 360 GHz*. Review of Scientific Instruments, 1999, 70 p. Available from: <https://doi.org/10.1063/1.1149977>
- [30] TOL, J. van, L.-C. BRUNEL and R. J. WYLDE. *A quasioptical transient electron spin resonance spectrometer operating at 120 and 240 GHz*. Review of Scientific Instruments, 2005, 76 p. Available from: <https://doi.org/10.1063/1.1942533>
- [31] HERTEL, M. M., V. P. DENYSENKOV and M. BENNATI. *Pulsed 180-GHz EPR/ENDOR/PELDOR spectroscopy*. 2005. DOI: 10.1002/mrc.1681.
- [32] KRŮŽ, R. *Tabulky materiálů a předvýrobků pro strojírenství*. Ostrava: Montanex, 2001. ISBN 807225042.
- [33] ROTH, A. *Vacuum technology*. Amsterdam: Elsevier Science Pub. Co., 1990. ISBN 978-0-444-86027-9.
- [34] O'HANLON, J. F. *A user's guide to vacuum technology*. 3rd ed. Hoboken, 2003. ISBN 9780471270522.
- [35] MICHAL, P. *Konstrukce nízkoteplotních ultravakuových rastrovacích sondových mikroskopů*. Brno, 2016. Ph.D. thesis. VUT, FSI.
- [36] JOUSTEN, K. a C. B. NAKHOSTEEN. *Handbook of vacuum technology*. WILEY-VCH. Weinheim, 2008. ISBN 978-3-527-40723-1. Available from: <http://www.gbv.de/dms/ilmnau/toc/562965394.PDF>
- [37] SOJKA, A. *Nízkoteplotní rastrovací tunelová mikroskopie*. Brno, 2017. Master's thesis. BUT FME.
- [38] *National Physical Labory: Kayen and Laby, Table of Physical and Chemical Constants* [online]. 2017 [cit. 2018-05-23]. Available from: [http://www.kayelaby.npl.co.uk/general\\_physics/2\\_3/2\\_3\\_6.html](http://www.kayelaby.npl.co.uk/general_physics/2_3/2_3_6.html)

- [39] *MatWeb: Material Property Data* [online]. 2011 [cit. 2018-05-23]. Available from: <http://www.matweb.com/index.aspx>
- [40] RIVIERE, L., N. CAUSSE and A. LONJON. *Specific heat capacity and thermal conductivity of PEEK/Ag nanoparticles composites determined by Modulated Temperature Differential Scanning Calorimetry: Polymer Degradation and Stability*. Elsevier, 2016, p. 98 - 104. ISSN 01326959. Available from: <https://www.sciencedirect.com/>
- [41] *Vespel S Line: Design Handbook* [online]. [cit. 2018-05-23]. Available from: <http://www.dupont.com/>
- [42] *Engineers EDGE: Engineering Book Store Roughness Comparators Drafting Supplies* [online]. USA, 2018 [cit. 2018-05-23]. Available from: [https://www.engineersedge.com/properties\\_of\\_metals.htm](https://www.engineersedge.com/properties_of_metals.htm)
- [43] HALLIDAY, D., R. RESNICK and J. WALKER. *Fyzika: vysokoškolská učebnice obecné fyziky*. Brno: VUTIUM, 2000. Překlady vysokoškolských učebnic. ISBN 80-214-1868-0.
- [44] PTC: Creo 4.0 [online]. [cit. 2018-05-23]. Available from: <https://www.ptc.com/en/cad-software-blog/download-creo-4-now>
- [45] CEITEC: Magneto-Optical and THz Spectroscopy [online]. Brno, 2018 [cit. 2018-05-23]. Available from: <http://spectroscopy.ceitec.cz/>
- [46] CHENG, X., Z. SONG, J. ZHANG et al. *Optimal coating solution for a compact resonating cavity working at Brewster angle*. 2016. Available from: <https://doi.org/10.1364/OE.24.024313>
- [47] BREWSTER, D. "On the Laws Which Regulate the Polarisation of Light by Reflexion from Transparent Bodies". London: Royal Society, 1815, 36 p. Available from: <http://www.jstor.org/stable/107362>
- [48] *Thomas Keating Ltd* [online]. UK [cit. 2018-05-23]. Available from: <http://www.terahertz.co.uk/>
- [49] *Stepper motors EMMS-ST: Festo* [online]. [cit. 2018-05-23]. Available from: [https://www.festo.com/net/SupportPortal/Files/212956/13\\_1-18%20-%20Stepper%20motors%20EMMS-ST\\_ENUS.PDF](https://www.festo.com/net/SupportPortal/Files/212956/13_1-18%20-%20Stepper%20motors%20EMMS-ST_ENUS.PDF)
- [50] SHIGLEY, J. E., C. R. MISCHKE and R. G. BUDYNAS. *Konstruování strojních součástí*. VUTIUM, 2010. ISBN 978-80-214-2629-0.

- [51] *NETWORK GRROUP s.r.o.* [online]. Brno, 2018 [cit. 2018-05-23]. Available from: <http://www.nwg.cz/>
- [52] LEE, D., P. R. HAYNES and D. J. SKEEN. *Properties of optical fibres at cryogenic temperatures*. 2001, p. 775-780. Available from: <https://doi.org/10.1046/j.1365-8711.2001.04630.x>
- [53] YUANMU, D., R. P. PANDIAN and R. AHMAD. Cryogenic fiber optic assemblies for spaceflight environments: design, manufacturing, testing, and integration. *NASA Goddard Space Flight Center*. USA, 2016, 16 p.
- [54] JAVOR, E. R. and T. ANDERSON. *Design of a Helmholtz Coil for Low Frequency Magnetic Field Susceptibility Testing*. USA, 1998, p. 912-917.
- [55] PATOČKA, M. *Vybrané statě z výkonové elektroniky –magnetické obvody ve výkonové elektronice, pulsní měniče s transformátorem*. Script.
- [56] RAMSDEN, E. *Hall-effect sensors : theory and applications*. Amsterdam: Elsevier Newnes, 2006, **2nd ed.**, 195 p. ISSN 978-0-75067934-3.
- [57] *NI PXIe-4610*. 2013. Available from: <http://www.ni.com/pdf/manuals/374189a.pdf>
- [58] *ANSYS: Electromagnetics* [online]. [cit. 2018-05-23]. Available from: <https://www.ansys.com/products/electronics>
- [59] *CST - Computer Simulation Technology: CST STUDIO SUITE* [online]. Dassault Systemes [cit. 2018-05-23]. Available from: <https://www.cst.com/products/csts2>
- [60] *Attocube: Attomotion* [online]. 2018 German [cit. 2018-05-23]. Available from: <http://attocube.com/attomotion/premium-line/anrv51/>
- [61] *MASTERBOND: Epoxy Adhesives for Cryogenic Applications* [online]. [cit. 2018-05-23]. Available from: <https://www.masterbond.com/>
- [62] LAMB, J. W. *Miscellaneous data on materials for millimetre and submillimetre optics*. Domaine Universitaire de Grenoble: Institut de Radio Astronomie Millimétrique, 1996, 36 p.



# APPENDIX

## CD with the CAD models.

Abbreviation	3D model
1.00 – CSH	Carousel Sample Holder
1.00 – RSH	Rotating Sample Holder
1.00 – PROBE	Probe